

https://dspace.org/

Evaluation of humic acids as potential acid catalysts for transalkylation

Skhonde, M P

2006-03-27
http://hdl.handle.net/10539/337

Downloaded from a DSpace repository. https://dspace.org/

EVALUATION OF HUMIC ACIDS AS POTENTIAL ACID CATALYSTS FOR TRANSALKYLATION

M P Skhonde

A research report submitted to the Faculty of Engineering and the Built Environment, University of the Witwatersrand, Johannesburg, in partial fulfilment of the requirements for the degree of Master of Science in engineering.

Johannesburg, 2004

DECLARATION

I declare that this thesis is my own work. It is being submitted for the Degree of Master of Science in Engineering in the University of the Witwatersrand, Johannesburg. It has not been submitted before for any degree or examination in any university.

_____

(Signature of candidate)

_____ day of _____ (year) _____

ABSTRACT

Transalkylation, a process of transfer of alkyl groups from one aromatic compound to another is carried out on acidic catalysts such as zeolites. The porous nature of zeolites is a prohibiting factor for transalkylation involving highly conjugated aromatic compounds. The study looks at the production of humic acids as well as their evaluation as potential acid catalysts for transalkylation.

Optimisation of the production of humic acids was carried out through determination of a suitable coal type using air oxidation. Slurry phase oxidation was used to enhance and optimise coal oxidation and the production of humic acids. From the characterisations and test reactions carried out, humic acids do show some catalytic properties; however the study also showed that the strength of the acid sites is not strong enough to induce transalkylation reactions. Investigations of using humic acids as catalysts for other reactions such as oxidative dehydrogenation of ethylbenzene to form styrene, is recommended.

DEDICATION

To my baby boy, born on the 2nd of August 2004

Njabulo Siphamandla Skhonde

ACKNOWLEDGEMENTS

I would like to thank my supervisors: Professor Rosemary Falcon and Professor Mike Scurrel for their assistance and support throughout the project. My gratitude also goes to Dr. Tjaart van der Waalt, Dr. Herman Louwrens, Dr. Humphrey Dlamini, William Tsatsi, Abram Aphane and Kgutso Mokoena from Sasol Technology R&D and Dr. Xin-Ying Liu from the University of the Witwatersrand for their continued support and assistance. Sasol Technology R&D for their financial assistance as well as providing the research facilities used to carry out the work.

CONTENTS **PAGE**

Declaration 1

Abstract 2

Dedication 3

Acknowledgements 4

Contents 5

List of Figures 8

List of tables 10

List of Symbols and nomenclature 11

1 INTRODUCTION 12

1.1 General Introduction 12

1.2 Background on acid catalysts 13

1.2.1 Zeolites as catalysts 15

1.2.2 Steric influence of zeolites 17

1.2.3 Applications of zeolites 18

1.3 Humic acids 19

Synthesis and characteristics 19

1.4 Aims of the study 21

2 EXPERIMENTAL 22

2.1 Introduction 22

2.2 The effect of coal type using air oxidation 22

2.2.1 Coal samples 22

2.2.2 Oxidation process 23

2.2.3 Extraction of humic acids 23

2.2.4 Characterization of products 24

Ultimate analysis 24

Functional groups determination 24
Carboxylic acids groups 25
Phenolic groups 26
Total acids 26
Infra-Red analysis 27
2.3 Slurry phase oxidation 27
2.3.1 Coal Samples 27
2.3.2 Oxidation process 27
2.3.3 Extraction of Humic Acids 29
2.3.4 Characterization of products 29
2.4 Acid catalysis characterisation on humic acids and zeolites 29
2.4.1 Elemental analysis and functional groups 30
2.4.2 Acidity characterizations 31
Acid strength and type of acid site using transmission FTIR 31
Amount/concentration of acid sites 31
2.4.3 Thermal analysis 32
Thermal stability- TGA 32
Detailed thermal analysis 32
2.5 Catalytic test reactions 32
2.5.1 Introduction 32
2.5.2 Experimental 33
Materials 33
Experimental Procedure 34

3 RESULTS & DISCUSSION 35

3.1 Introduction 35
3.2 Effect of Coal Type using air oxidation 35
3.2.1 Characterization of the feed 35
3.2.2 Oxidation product yields 36
Yields of oxidised coal 36

Yields of Humic acids 38
3.2.3 Characterizations 40
Ultimate analysis 40
Functional groups determination 45
Carboxylic acid groups 47
Phenolic acid groups 49
IR analysis of Waterberg coal products 50
3.2.4 Conclusions 51
3.3 Slurry phase oxidation 52
3.3.1 Oxidation products yields 53
3.3.2 Characterizations 54
Ultimate analysis 54
Functional groups determination 55
3.3.3 Conclusions 56
3.4 Acid catalysis characterizations on humic acids and zeolites 56
3.4.1 Strength and type of acid sites 56
3.4.2 Amount/concentration of acid sites 59
3.4.3 Thermal analysis 61
TGA analysis 61
Detailed thermal analysis of humic acids 62
3.4.4 Conclusions 66
3.5 Catalytic test reactions 67
3.5.1 Introduction 67
3.5.2 Results and discussion 67
3.5.3 Conclusions 72
4 CONCLUSIONS AND RECOMMENDATIONS OF THE STUDY 73
APPENDICES 75
REFERENCES 81

LIST OF FIGURES **PAGE**

1.1 Acid sites in zeolites 12
1.2 Representative structure of humic acids 13
Scheme 1.1: Acid catalysed transalkylation between benzene and xylene to produce toluene 15
1.3 Structure of zeolites showing charge associated with the building units 16
1.4 Reactants and products selectivity with zeolites 17
1.5 Transition state selectivity with zeolites 18
1.6 Coal oxidation process and production of humic acids 20
2.1 Simplified flow sheet for slurry phase oxidation and product work-up 28
2.2 Diagram of an autoclave used for slurry phase oxidation 29
3.1 The yields of oxidised coal with the extent of oxidation 38
3.2 Dependence of humic acids yields on the reaction time of oxidation 39
3.3 Humic acids extracted from the three coal samples 40
3.4 Carboxylic acid groups distribution for Waterberg, Twistdraai and Syferfontein coals oxidised at 60°C 47
3.5 Carboxylic acid groups distribution for Waterberg, Twistdraai and Syferfontein coals oxidised at 150°C 48
3.6 Phenolic acid groups distribution for Waterberg, Twistdraai and Syferfontein coals oxidised at 60°C 49
3.7 Phenolic acid groups distribution for Waterberg, Twistdraai and Syferfontein coals oxidised at 150°C 50
3.8 FTIR spectra of Waterberg oxidation products 51
3.9 Oxidation products yields for Waterberg coal slurry phase oxidation 53
3.10 The behaviour of functional groups with increased temperature of reaction for slurry phase oxidation 55
3.11 FTIR spectra of (A) H-Mordenite and (B) H-Y zeolite after pyridine adsorption 57

3.12 FTIR spectra of (A) H-mordenite and H-Y zeolite in the hydroxyl region 58
3.13 DRIFTS spectra of humic acids 59
3.14 Concentration of H^+ ions on the catalysts samples 60
3.15 TGA plot for the catalysts samples 61
3.16 Mass loss experienced with thermal treatment of humic acids 62
3.17 Functional groups on humic acids after thermal treatment 63
3.18 FTIR spectra with thermally treated humic acids samples 64
3.19 The atomic ratio (C/H) with humic acids thermal treatment 65
Scheme 2 Ethylbenzene disproportionation 67
3.20 Ethylbenzene conversion at different temperatures 68
3.21 Yields of products at different temperatures 70
Scheme3 Formation of 1-phenyl ethanol and 1-phenyl ethanone from ethylbenzene 71
Scheme 4 Styrene formation from 1-phenyl ethanol and 1-phenyl ethanone 71

LIST OF TABLES **PAGE**

2.1 Elemental analysis and acid content of humic acids extracted from Waterberg coal oxidised at 180 °C 30
3.1 Petrographic parameters of coals used 36
3.2 Ultimate analysis of Twistdraai coal products 42
3.3 Ultimate analysis of Syferfontein coal products 43
3.4 Ultimate analysis of Waterberg coal products 44
3.5 Functional groups obtained for oxidised products (air oxidation) 45
A1 Yields of extracted humic acids 75
A2 Results of slurry phase oxidation 76
A3 Functional groups determination for slurry phase oxidation 77
A4 Integral results of Lewis and Bronsted acid sites (1350-1700 cm-1 region) 77
B1 Molar composition of the products obtained for ethylbenzene disproportionation at 180°C 78
B2 Molar composition of the products obtained for ethylbenzene disproportionation at 200°C 78
B3 Molar composition of the products obtained for ethylbenzene disproportionation at 250°C 79

C Determination of the amount of H+ ions per gram of dry resin 79

LIST OF SYMBOLS AND NOMECLATURE

Vs	Volume of a titrate (ml) used with the coal
Vb	Volume of a titrate (ml) used for the blank
N	Concentration of the solution (Mol)
n	number of moles of a molecule
Fig.	Figure
a.r	as received
d.a.f	dry ash free
ROM	Run of mine
FT-IR	Fourier Transform Infra red
FA	Fulvic acids
RoVmr	Mean random reflectance value
GC-MS	Gas Chromatography- Mass Spectroscopy
h	Hours
l	litres
min	minutes

1 INTRODUCTION

1.1 General Introduction

Transalkylation is a process of transfer of alkyl groups from one aromatic compound to another. This process is carried out using a suitable acid catalyst [1]. Zeolites have been widely used for transalkylation of simple/light aromatic compounds such as benzene and their derivatives. Zeolites posses a number of advantages over other acid catalysts which include the fact that they can be applied at high temperatures, their porous nature allows for shape selectivity, they have high internal surface area and they have ion-exchange properties as well as high adsorption capacities [2].

The acidic protons of zeolites are derived from the OH groups attached to a Si- and Al as shown in figure1.1.

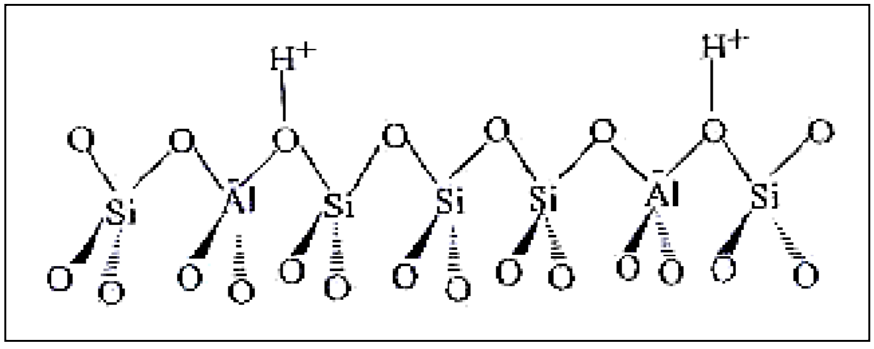


Figure 1.1: Acid sites in zeolites [4]

Transalkylation involving bulky molecules such as diethylbenzenes uses modified zeolites which are multi-dimensional with large pore sizes. Harsher reaction conditions, such as high temperatures, are required to carry out these reactions [3]. Due to the porous nature of zeolites, there are steric limitations with increasing molecular size and aromatic conjugation in accessing active sites in the catalyst channels where alkyl-transfer reactions takes place. As a result limited work has been reported on transalkylation involving more conjugated aromatic compounds such as naphthalene, anthracene, pyrene,

etc. A challenge is to investigate other solid acid catalysts where the steric hindrance is lifted while at the same time the active sites density and the acid strength are not compromised.

Humic acids which are produced by extraction from oxidized coal are thought to have the required properties to catalyze alkyl transfer reactions as they have acidic phenolic as well as carboxylic acids groups that are acidic and they have ion-exchange properties.

They undergo ion-exchange reactions whereby H^+ ions of the carboxylic acids and phenolic acids are easily donated because of their acidic nature. Figure 1.2 shows the structure of humic acids with the functional groups that they possess, as proposed by Stevenson [5].

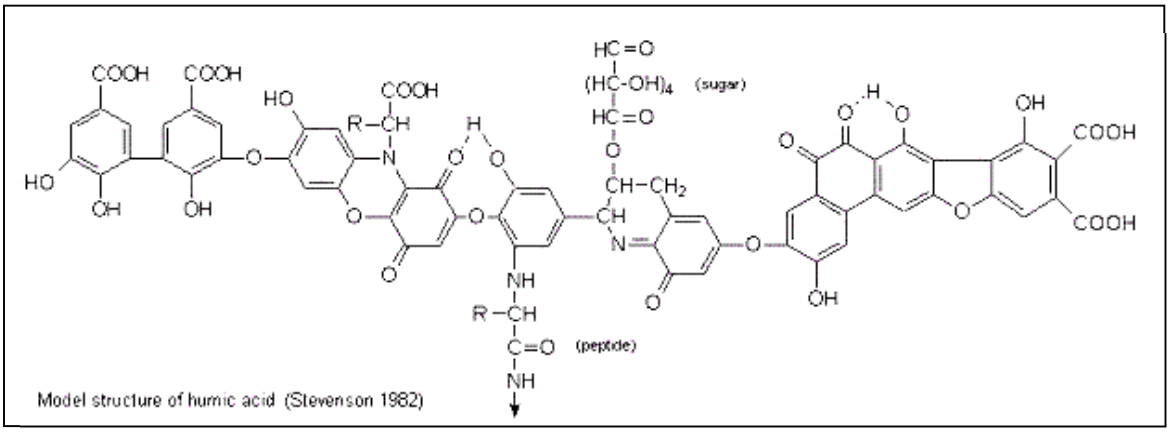


Figure 1.2: Representative structure of humic acids [5]

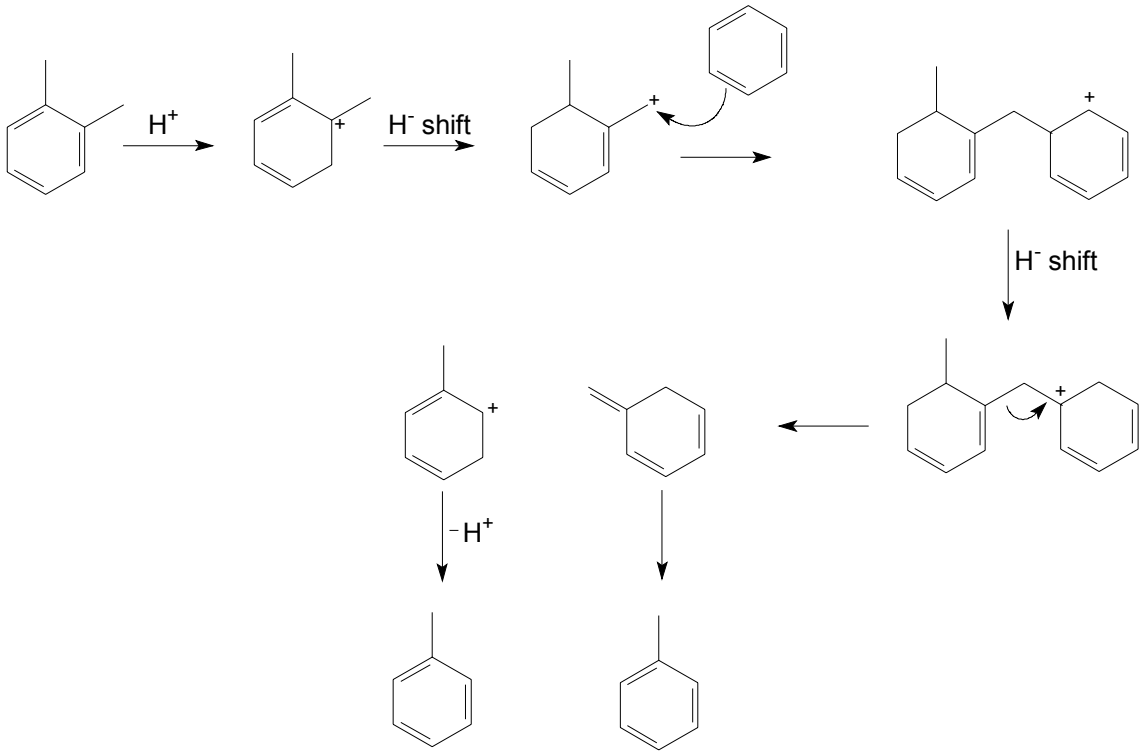
1.2 Background on acid catalysts

Catalysis by acids generally proceeds via cycles involving hydrogen transfer reactions. In solution, solvent molecules such as water often play a role; e.g. by interacting strongly with reaction intermediates and/or by being donors of protons. Reactions catalysed homogeneously are also catalysed by solid acids (heterogeneously), but heterogeneous reactions usually take place in the absence of solvents and at much higher temperatures than are practical homogeneously.

General acid catalysis predominates in solid acid catalysis. However due to the fact that typical solid acids such as metal oxides incorporates both a spectrum of proton donor groups such as OH groups (Brønsted acid sites) and a spectrum of electron pair acceptor groups (Lewis acid sites) with various strengths, catalytic sites remain almost unidentified. Thus although there may be simple relationships between catalytic activities and easily measured properties characterizing acidity, they often do not provide much insight into the nature of the catalytic sites or the reaction mechanisms.

There exists a large variety of solid acid catalysts, i.e. natural clay minerals, mounted acids (H_3PO_4 mounted on diatomaceous earth), cation exchange resins (Nafion), oxides (alumina) and mixtures of oxides (silica-alumina), salts ($MgSO_4$), and zeolites. The acidity of these solids even within a class can be completely different: Some acids can be considered as superacids while others have a very reduced acid strength [4].

Transalkylation between benzene and xylene to form toluene is outlined in scheme 1 where the reaction mechanism highlights the role of acid catalysts in such transformations.



Scheme 1: Acid catalysed transalkylation between benzene and xylene to produce toluene [6]

1.2.1 Zeolites as catalysts

In the early days, liquid Friedel-Crafts and HF-BF_3 systems were commonly used as catalysts for transalkylation. In modern technology, zeolite catalyst systems are predominant. Transalkylation processes are normally catalysed by porous zeolites which can be used for toluene disproportionation. Zeolites are microporous, high-internal surface area crystalline materials with an open, three-dimensional framework consisting of tetrahedral AlO_4^{-5} and SiO_4^{-4} units linked through shared oxygen (figure 1.3).

Owing to their unique properties in ion-exchange, adsorption capacity and catalytic activity, zeolites have been widely used as adsorbents, molecular sieving agents, catalysts support and catalysts for a variety of different chemical reactions. Zeolites are now widely used in the petrochemical industry, for example, in the selective synthesis of

chemical intermediates and numerous other industrial processes such as the MTG (methanol to gasoline) [7].

Zeolites have also been modified by isomorphous substitution of silicon and aluminium by incorporating other atoms such as titanium, iron, gallium, boron, phosphorous, etc. in the framework. The number of synthetic zeolites with new structural morphologies grows rapidly with time. Zeolites are members of a family of minerals called tectosilicates, which includes dense-phase materials such as the feldspars and the various forms of silica. There are 40 known naturally occurring zeolites and more than 150 synthetic ones. Zeolite structures can be visualized by taking a neutral SiO_2 framework and isomorphously substituting it with AlO_2^-.

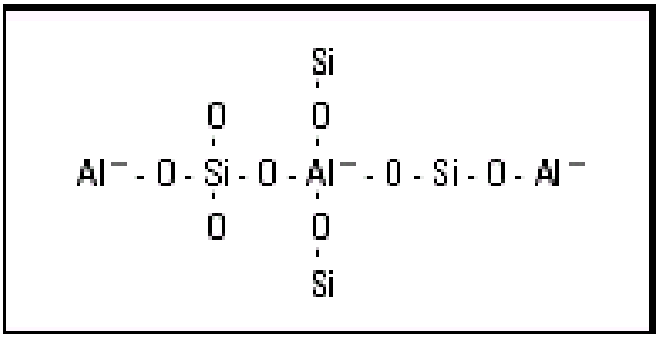
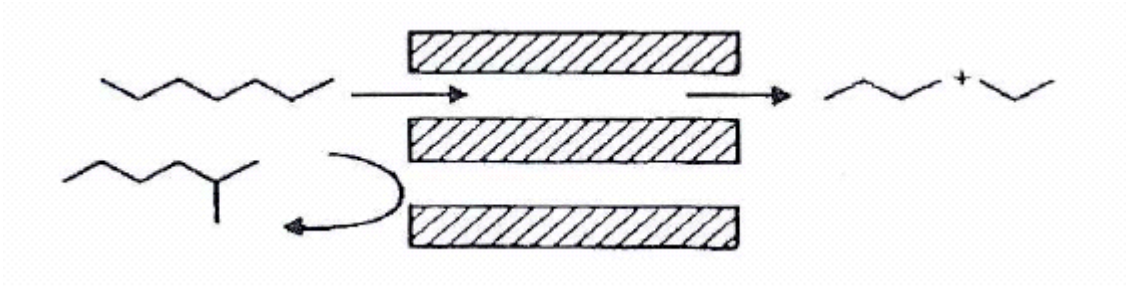


Figure 1.3: Structure of zeolites showing charge associated with the building units

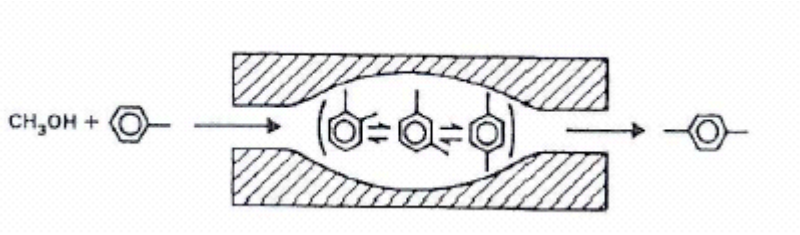
The resulting structure (Figure 1.3) then exhibits a net negative charge on the framework aluminium. This negative charge is balanced by cations (for instance, Na^+, K^+, or NH_4^+) that reside in the interstices of the framework. Many of these cations are mobile and free for exchange. This ion-exchange property accounts for the greatest volume use of zeolites today.

1.2.2. Steric influence of zeolites

Catalysts such as zeolites with pore diameters about equal to molecular dimensions can exert strong steric influences in catalysis; the phenomena are referred to as shape selective catalysis. Narrow pores can exert strong repulsive forces on reactant molecules that just fit in them, and in the limiting case molecules that are too large to fit are excluded from any catalytic site in the interior catalyst volume. Reactant shape selectivity takes place when some reactants are sieved out and others fit in the pores. Product shape selectivity occurs when some products formed in the pores are too large to migrate readily through the apertures and out of the pores; thus their rate of entry into the product stream is hindered relative to that of any of other products, these are transport effects (figure 1.4 &1.5).



Reactants selectivity



Product selectivity

Figure 1.4: Reactants and products selectivity with zeolites

Restricted transition state shape selectivity is not a transport effect; it directly affects the reaction mechanism. It occurs when a transition state is large enough that it is subject to

steric repulsion because of contact with the catalyst pore walls, which can retard the conversion of one reactant relative to that of another that forms a smaller transition state.

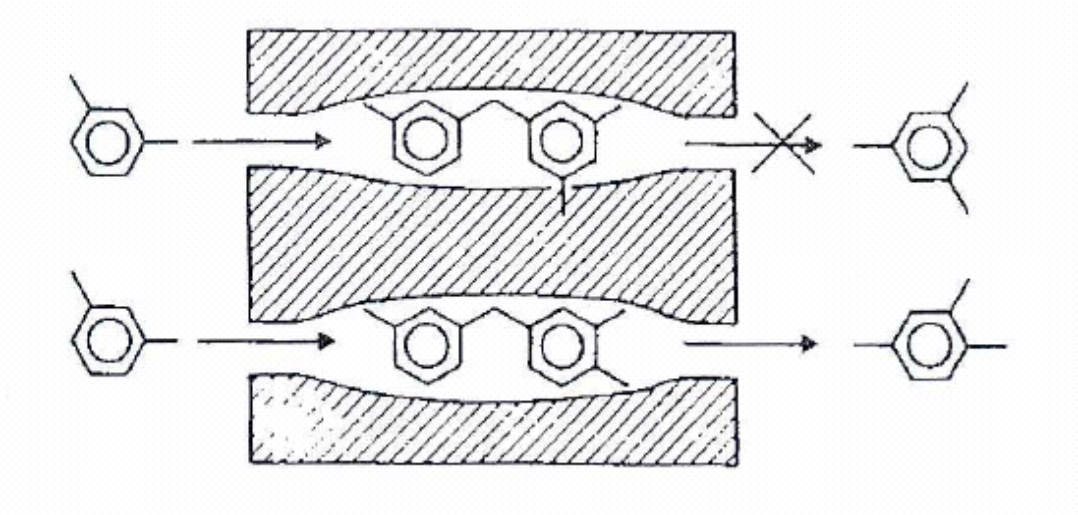


Figure 1.5: Transition state selectivity with zeolites

Another kind of shape selectivity has been inferred from the observation that some reactants and transition states can be stabilized relative to smaller species because of a good fit in the catalyst pores, which maximizes attractive van der Waals forces. This effect is absent in larger pores. It is attributed to a propitious steric fit suggestive of the lock and key fit that in part explains the efficiency of enzyme catalysts.

1.2.3 Applications of zeolites

Zeolites have seen a wide range of applications, both industrially and environmentally. Industrially they have found a wide application in petroleum refining (catalytic cracking, isomerisation and dewaxing), synfuels production, oligomerisation and alkylation reactions, or as catalysts supports [8].

Other applications of zeolites include waste water treatment, removal of radio active metals from nuclear effluent, animal feed supplements, soil improvement, photochemical

and electrical reactions, separation of gases and liquids and as adsorbents and detergent builders.

1.3 Humic acids

Humic substances are primarily the microbiological transformation products of lignin and other plant detritus. Humic acids from coal can be produced by the oxidation of coal under controlled conditions [9]. Coal humic acids may be defined as dark coloured substances derived from coals, which are soluble in aqueous alkali but insoluble in acid. They occur naturally in some lignite and brown coals, but little or no alkali soluble material is present in bituminous coals.

Less mature coals, including brown coals and lignites, may contain molecules with significant amounts of acidic groups, substantial proportions of which may be extracted into aqueous alkali media as alkali metal humates. However mild oxidations of mature coals result in the formation of regenerated humic acids or ulmins, which fall within the above definition [10].

The amount of humic acids in coal depends on the degree of maturity (rank) of that coal, as well as on the nature of coalification process involved during the formation of the coal [11]. Since humic acids themselves can be oxidized fairly readily to water soluble carboxylic acids, conditions of oxidation have to be optimized to gain maximum humic acids yields. Dilute aqueous alkali appears to be the most favoured extractant, since it is selective in dissolving only acidic material, leaving both the mature coal substance and inorganic mineral matter undissolved [12].

Synthesis and characteristics

Humic acids are organic components extracted from oxidized coal using a suitable base. Oxidation takes place when coal is exposed to an oxygen rich atmosphere. The oxygen is incorporated in the coal surface through chemisorption to give different oxygen bearing

functional groups. The process is known to be affected by temperature and time of exposure.

Different methods can be used to accomplish the incorporation of oxygen. One of the methods that can be used is the non-catalytic oxidation of water slurried coal with oxygen, which is a promising route towards the production of oxihumic and oxifulvic acids [13]. The produced humic acids are called regenerated humic acids from their origin as indicated in figure 1.6.

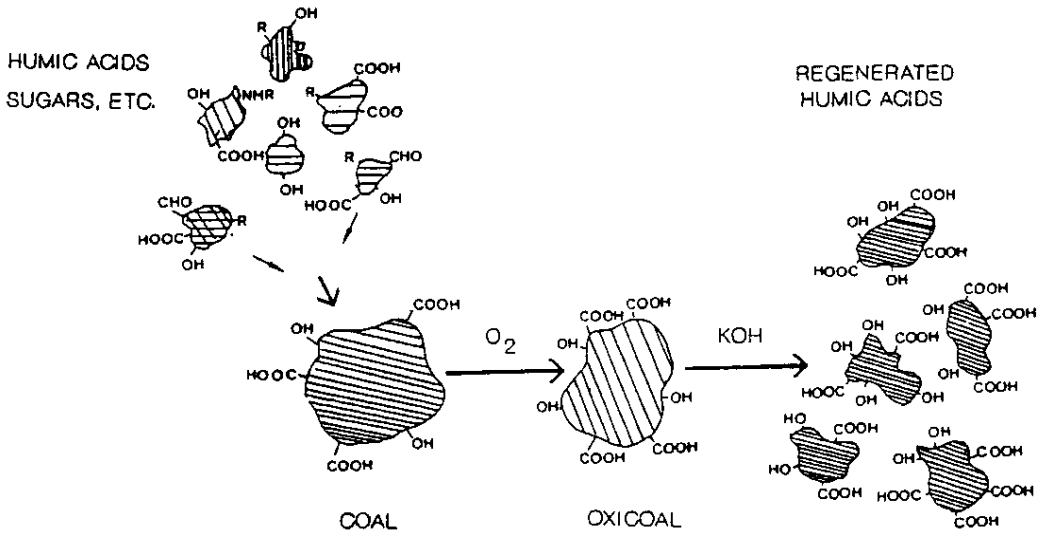


Figure 1.6: Coal oxidation process and the production of humic acids

Another method that is widely reported is oxidation using nitric acid. In Japan some thousand tons per year of nitro humic acids are produced from low rank coals and commercialized in the local market for agricultural applications which include soil stabilization, micro element transportation, plant growth stimulation, herbicide control as well as waste water application [14].

1.4 Aims of the study

With the production of humic acids from coal, it is important to optimize the production conditions which are affected mainly by the type of coal used, as well the oxidation method employed. One of the objectives of the study was to optimize the conditions for the production of humic acids by investigating the different types of South African coals, as well as the different oxidation methods. Different coal types will give different activities (reactivity) due to differences in their organic constituents such as the maceral compositions. For the study carried out, coals with different vitrinite and mineral matter contents were evaluated for their ability to produce humic acids.

The extent of oxidation can also be affected by the oxidation methods that are used. Some oxidation methods are found to be more effective than others due to the conditions associated with them. The abilities of the different oxidation methods seem to dictate the extent of oxidation as well the production of humic acids.

The second objective of this investigation was to evaluate the ability to utilize humic acids as potential catalysts for transalkylation. This was carried out through characterization of the humic acids which was followed by test reactions for transalkyaltion. One of the important characterizations that needed to be carried out was the thermal analysis since the thermal stability will determine temperatures at which the humic acids can be applied as catalysts. The comparison of the properties of humic acids was carried out by comparison with zeolites (Y-zeolite and mordenite), through characterizations and test reactions.

2. EXPERIMENTAL

2.1 Introduction

The production of humic acids was carried out through oxidation of coal (regeneration). The first step was the optimization of the reaction conditions (i.e. the type of coal and oxidation method) through screening of different South African coals as well as different oxidation methods. Once the best oxidation conditions were established the humic acids produced were subjected to catalytic characterizations together with zeolites for comparison. Other characterisation such as thermal analysis was also carried out; this was followed by test reactions involving ethylbenzene. This chapter highlights all the experimental work carried out for the production of humic acids, their characterisation as well as test reactions carried out with humic acids as catalysts.

2.2 The effect of coal type using air oxidation

2.2.1 Coal samples

The first part was the investigation of the effect of different types of coals on the production of humic acids using air oxidation. The coals that were used were Sasol coals (Twistdraai and Syferfontein), as well as the coal from Waterberg coal mine of ISCOR. Samples were conditioned by putting them under inert (N_2) atmosphere for 1 to 2 weeks. The coals used were ground to a particle size of -150µm. This particle size was chosen because it has been reported that -150µm is the maximum particle size at which sufficient oxidation can be achieved [15].

Petrographic analysis was carried out on the three coal samples to determine the vitrinite content and the rank, as these have an impact on the reactivity of coal in a sense that, as the rank increases, the air dried moisture content tends to decrease and the percentage carbon in the coal increases. However, changes also occur in the petrographic characteristics of the coal, and coal of the same rank can have different macerals

compositions leading to different coal behaviour or characteristics brought about by different carbon content [16].

Ultimate analysis as well as the determination of functional groups was carried out on all the coals for comparison with the products.

2.2.2 Oxidation process

The oxidation method employed for the investigation of the effect of the different coal type is air oxidation. The oxidation was carried out in an oven by spreading the finely ground coal in a thin layer on an aluminium tray, while allowing a free flow of air over the coal surface. The method was recently used by Ashmin et al. [17] for studying the chemical changes accompanying oxygenation of coal by air.

The coals were oxidized at 60±5ºC as well as at 150±5ºC for different time periods ranging from 3 h to 380 h. These temperatures were chosen because they have been used for similar processes [17, 18, 19].

2.2.3 Extraction of humic acids

The extraction procedure used was taken from the work that was reported by Louwrens [20]. 10 g of the oxidized coal was added into a solution of sodium hydroxide (10g in 400cm^3 of distilled water). The mixture was refluxed at 100ºC for 5 h. The reaction mixture was centrifuged at 2500 rpm for 15 minutes and the supernatant (humic acid in solution) was collected. The residue was washed with 0.1 M NaOH (2×200cm^3) followed by 400cm^3 distilled water. The filtrate was decanted to the supernatant. The residue was also washed with 200cm^3 of 10%HCl followed by 200cm^3 of distilled water. The residue was dried at 100ºC and collected for proximate and ultimate analysis for mass balance.

The humic acid solution was acidified with HCl until a pH of 2 was achieved; the process resulted in the precipitation of humic acid. The mixture was centrifuged at 2550rpm for

15 min and the precipitate was washed with small amounts of distilled water and centrifuged at 2500 rpm for 15 min. The humic acids product was dried overnight at 100ºC.

2.2.4 Characterization of products

The oxidized coal products were characterized using ultimate analysis and surface sensitive techniques that indicated oxidation and types of oxygen groups on the coal surface (i.e. the determination of carboxylic groups, the phenolic groups, as well as total acid groups). Infrared spectroscopy was applied to investigate the surface composition of the oxidised coal products.

Ultimate analysis

The samples were all analyzed for the elemental composition, that is, carbon, hydrogen, nitrogen, sulphur and oxygen. Elemental compositions (C, H, S and N) were determined by combustion analysis using a LECO elemental analyzer and oxygen was determined by difference. This was carried out to establish the extent of oxidation at different reaction conditions.

Functional groups determination

This determination was carried out to establish the manner in which the oxygen binds to the coal surface. Oxygen can bind on the coal surface forming either carboxylic acid groups (-COOH) and/or phenolic groups (OH). The total acids were also determined as described below. The procedures used were taken from the work done by Schnitzer and Khan [21].

Before any of the determinations, the coals were treated as follows:
About 10g of coal was added to 500cm^3 of a 1 mol/dm^3 HCl solution and stirred for a period of 24 h in order to hydrolyze all the carboxylic salts to the corresponding acid

form. Excess water was removed from the sample by filtration, and acid removed from the sample by soaking in distilled water. The product was then dried in a vacuum oven at 100ºC for a period of 6 h. A correction was made regarding the reduction in ash content following the removal of the carbonate minerals.

Carboxylic acid groups

Carboxylic acid groups were determined using ion-exchange reactions with calcium acetate; the concentration of the acetic acid formed is determined titrimetrically against a standard solution of sodium hydroxide. The reaction scheme for the ion-exchange is shown below:

$$RCOOH + 0.5\ Ca\ (OOCCH_3) \rightarrow RCOO\ (0.5Ca) + CH_3COOH$$

About 300mg of the dried coal, which was pre-treated as shown above, was added into a beaker together with a solution of 10 cm^3 of 0.5 mol/dm^3 calcium acetate and 50 cm^3 of deionised water, the beaker was sealed under nitrogen and the mixture was stirred for a period of 18 hours. After filtration, the sample was washed with small quantities of deionised water and the filtrate was titrated against a standard 0.02 mol/dm^3 sodium hydroxide solution using phenolphthalein as an indicator. The amount of carboxylic acids was then calculated in milli equivalent per gram of carbon using the formula:

$$\text{Carboxylic acids} = \frac{\{(Vs-Vb) \times N(NaOH)\} \times \{\%C \text{ in oxicoal}\}}{(\text{mass of coal})\ (100)}$$

Where: V_s = volume of base used with the coal (ml)

V_b = Volume of base for the blank (ml)

N (NaOH) = concentration of NaOH (0.02 mol/l)

Phenolic groups

Phenolic groups were determined from the amounts of the total acid groups and carboxylic acid groups, by taking the difference of the two. It was reported that the sum of carboxylic acid groups and the phenolic groups equals the total acid groups in the coal [21,22].

Total acids

The method used involves the reaction between excess barium hydroxide and the organic groups present. The reduction in barium hydroxide concentration was determined titrimetrically against a standardized hydrochloric acid solution. The reactions involved are shown in the scheme below:

1) $ROH + RCOOH + nBa(OH)_2 \rightarrow 0.5\,(RCOO)_2Ba + 2H_2O + 0.5(RO)_2Ba + (n-1)\,Ba(OH)_2$

2) $(n-1)Ba(OH)_2 + 2(n-1)HCl \rightarrow (n-1)BaCl_2 + 2\,(n-1)\,H_2O$

About 1g of the dried coal which was pre-treated as described in 2.2.4 was accurately weighed and added to a solution containing 2g of barium hydroxide in 40 cm^3 of double deionised water. The reaction mixture was stirred for 24 h under a nitrogen atmosphere, filtered and the coal residue washed with small quantities of distilled water in order to remove all the barium hydroxide present. The filtrate was titrated against a standardized 1mol/dm^3 HCl solution using bromothymol blue as an indicator. The formula that was used to calculate the total acid groups in milli equivalent per gram of carbon is:

$$\text{Total acid groups} = \frac{\{(Vb - Vs) \times N(HCl)\} \times \{\%C \text{ in oxicoal}\}}{(\text{mass of coal})\,(100)}$$

Where: Vs = volume of base used with the coal (ml)

Vb = volume of base for the blank (ml)

N (HCl) = concentration of HCl (1 mol/l)

Infrared analysis

The oxidation products and extracted humic acids were characterized using infrared spectroscopy. This was carried out in order to study the nature of functional groups in the oxidised coal products using potassium bromide (KBr). A spectrum of KBr was recorded followed by the recording of KBr with humic acid or coal (1.6g) which was pressed into pellets made from KBr (about 250mg). The difference spectrum was then interpreted as the spectrum of the humic acids or coal sample.

2.3 Slurry phase oxidation

2.3.1 Coal Samples

The coal that was used for slurry phase oxidation was obtained from Waterberg mines of ISCOR. The coal was a Run-of-Mine (ROM) product with a particle size of -150µm used as mentioned in section 2.2.1.

2.3.2 The oxidation process

The process of producing humic acids through oxidation of coal is shown in the schematically in figure 2.1.

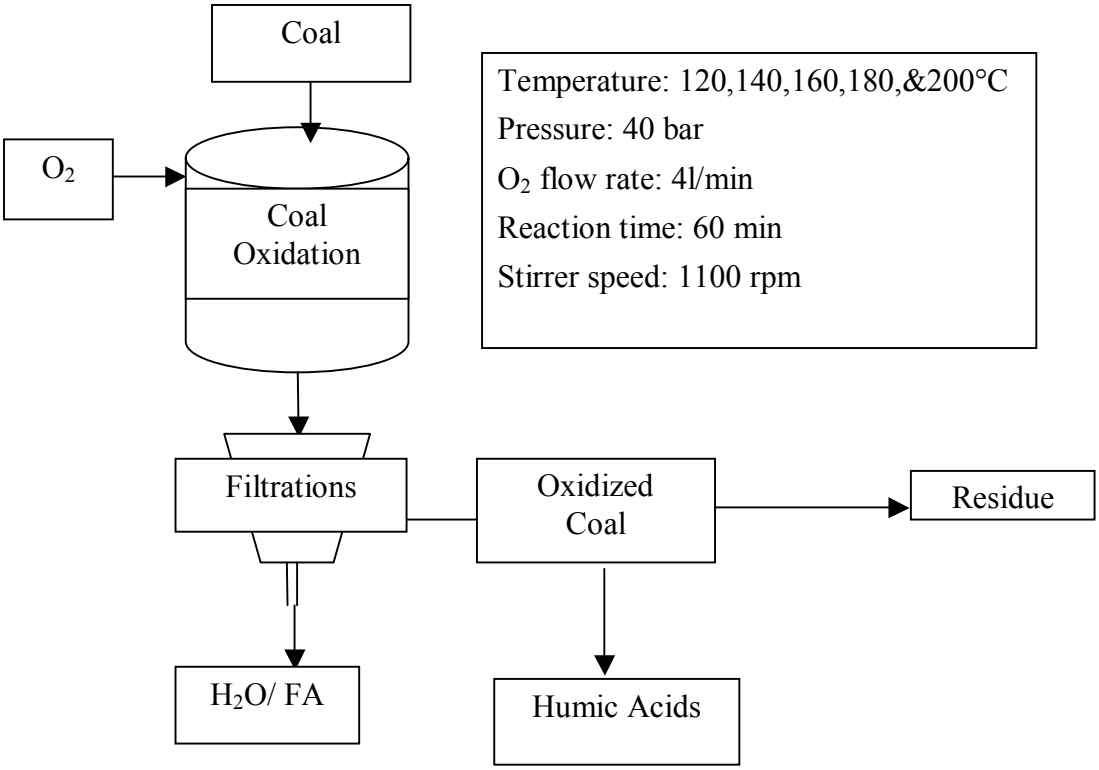


Figure 2.1: Simplified flow sheet for wet coal oxidation and product work-up.

The oxidation experiments were carried out in a 2 l autoclave (figure 2.2), equipped with external heating elements for initial heating up, an internal cooling coil for temperature control during a chosen reaction period and subsequent rapid cooling down, and a variable speed, magnetically driven Rushton-type stirrer for proper oxygen transfer.

In a typical experiment a well stirred (1100 rpm) slurry of 420g of -150µm Waterberg ROM coal and 700ml of water is preheated under constant pressure (40bar). When the desired temperature is reached (120, 140,160, 180, and 200°C), the let-down valve is set to permit the required oxygen flow rate (4 l/min). Due to the exothermic nature of the reaction, the external heating switches off automatically and intermittent cooling is required to maintain a constant temperature. When the desired reaction period (1 h) has elapsed, the oxygen flow is stopped and the temperature is decreased by operating the cooling coil at maximum capacity. This oxidation method was successfully used for oxidation by Dekker et al [23] and Bergh et al [24].

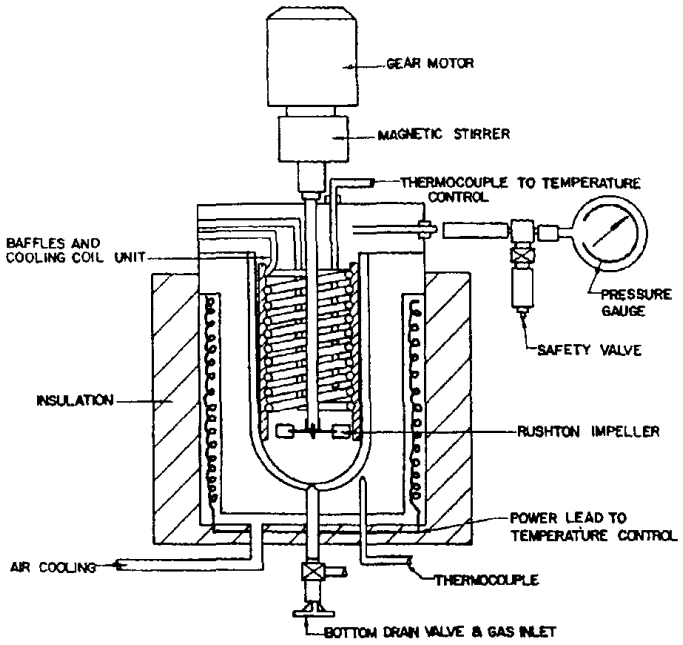


Figure 2.2: Diagram of autoclave used for slurry phase oxidation

2.3.3 Extraction of humic acids

The method for extraction of humic acids is described in section 2.2.3.

2.3.4 Characterization of products

The products obtained from oxidation and extraction of humic acids were characterized using the methods discussed in section 2.2.4.

2.4 Acid catalysis characterizations on humic acids and zeolites

After the optimization of the oxidation conditions it was decided that humic acids are extracted from the coal samples oxidized at 180°C. The oxidation conditions employed were also found to be optimum after the work that was done by Louwrens et al [22].

Humic acids were extracted from the samples obtained under these conditions, using extraction methods that are capable of extracting only the humic acids from the coal samples [20, 25]. Humic acids were characterized for their catalytic properties. Similar characterisations were also carried out on two zeolites types namely mordenite and Y-zeolite. The characterizations were carried out for comparison of humic acids with zeolites for their catalytic behaviour since these zeolites (mordenite and Y-zeolite) have been widely used for transalkylation reactions. [26,27, 28,29,30].

Y-zeolite and mordenite were received from Sued-Chemie. The Y-zeolite was received in a Na-form and was transformed to H-form using ion-exchange reactions followed by calcination of the product. Mordenite was received in an H-form. All the catalysts were milled to -150μm before characterization.

2.4.1 Elemental analysis and functional groups

The humic acids produced from coal oxidized at 180°C were characterized for elements and functional groups in order to establish the chemical compositions (table 2.1). Elemental compositions (C, H, and N) were determined by combustion analysis using a LECO elemental analyzer and oxygen and sulphur were determined by difference.

The carboxylic acids content and total acid content were determined by the method of Schnitzer and Khan [21].

Table 2.1: Elemental analysis, acid content of the humic acids extracted from Waterberg coal, oxidized at 180°C.

Elemental analysis (wt %)d.a.f.				Acidic content (meq g^{-1})		
C	H	N	S + O_{diff}	COOH	OH	Total acid
49.24	3.16	1.29	46.31	0.65	5.33	5.98

2.4.2 Acidity characterizations

The acidity of an acid catalyst is a measure of the number, nature, strength, and density of acid sites. The determination of the type of acid sites (as these can either be Bronsted or Lewis acid sites), can be done using infrared spectroscopy of different probe molecules such as pyridine, ammonia, carbon monoxide, etc. In this study pyridine was used as a probe molecule. This molecule clearly distinguishes the type of acid sites (i.e. Bronsted at 1545 cm^{-1} and Lewis at 1450 cm^{-1}). Pyridine FTIR is also sensitive to the strength of the Lewis acid sites. Increase in the strength of the Lewis acid site results in the shift of the Lewis acid site peaks to higher frequencies and vice versa.

Acid strength and type of acid sites using transmission FTIR

Humic acids and the selected zeolites were characterized for acid strength and type of acid sites using FTIR measurements of adsorbed pyridine as a probe molecule. Since humic acids are not IR transparent, DRIFTS was used, where the sample was mixed with KBr, finely ground, and then put into the DRIFTS cell. The samples were heated up at 200°C under nitrogen for 4 hours to remove moisture and any other organic molecules that might be adsorbed. Then the sample was cooled down to 40°C. Pyridine (0.5ml) was vaporized at 200°C and injected into the system. Adsorption was allowed to equilibrate for 5 min prior to spectra being recorded. Pyridine injection was bypassed for desorption for 1 h at 40°C then at 100°C and 200°C, spectra was recorded during desorption.

Amount/concentration of acid sites

The number of acid sites was determined using standard acid base titration reactions, where the product was titrated against a suitable base; in this case potassium hydroxide was used. The procedure is as described in appendix C:

2.4.3 Thermal analysis

Thermal stability- TGA

Humic acids extracted from coal were subjected to thermal analysis using thermogravimetric analysis (TGA). These were characterized using TGA together with the selected zeolites for comparison.

Detailed thermal analysis on humic acids

The results obtained for the analysis with TGA analysis showed a mass loss that was experienced with humic acids as the temperature of exposure was increased, therefore it was necessary to carry out a detailed thermal analysis. Thermal analysis of the humic acids was carried out to establish the impact of the mass loss on the chemical structure of the humic acids. This was carried out by treatment of the humic acid samples at different temperatures (200, 400, 600, 800, 1000°C), using a furnace under nitrogen atmosphere.

The behaviour of acidic functional groups with increased temperatures was monitored. This was achieved by analysis for carboxylic as well as the phenolic acid groups (section 2.2.4). Total acids were also determined for the different humic acids samples (section 2.2.4). Infrared spectroscopy was also used for the characterization of the functional groups on the humic acids (section 2.2.4). The distribution of carboxylic acids in relation to phenolic acids was investigated in order to establish the effect of increasing temperature on their stability against decomposition.

2.5 Catalytic test reactions

2.5.1. Introduction

The disproportionation of ethylbenzene to benzene and diethylbenzene is an acid catalysed reaction which readily occurs on a great variety of acid catalysts. This reaction

is an interesting model reaction, first studied by Karge et al. to characterise zeolites in their acid forms [32,33].

Another well known reaction carried out with ethylbenzene is the production of styrene. This is carried out through oxidative dehydrogenation (ODH) of ethylbenzene at high temperatures (above 600°C) with promoted iron oxide catalysts in the presence of steam [34]. The major drawback of this process is that dehydrogenations are reversible reactions, therefore imposing a thermodynamic limitation to the conversion which can be attained (~50%).

Using other catalysts such as zeolites, alumina and phosphates for styrene production it was observed that there is a formation of a coke layer, which was found to be the real catalytic surface [35,36, 37,38]. This lead to studies on using carbon material as catalysts for the ODH of ethylbenzene. A lot of studies have been carried out on the use of activated carbon as catalysts for ODH of ethylbenzene to form styrene [28,29,30]. Coal was used as a catalyst for ODH of butane to form butene by Maldonaldo-Hodar et al. [39]. In this section, transformation of ethylbenzene using humic acids as catalysts was attempted. The aim was to carry out transalkylation or disproportionation of ethylbenzene, and also to observe any other possible reactions that might be catalysed by humic acids e.g. ODH.

2.5.2 Experimental

Materials

The humic acids used were synthesized as described in section 2.2.3, and they were characterised as described in section 2.4. Ethylbenzene (99% pure) was supplied by Sigma-Aldrich. The ethylbenzene solution was not purified to remove oxygenates such as 1-phenylethanone, and 1-phenylethanol. This was done in order to observe any other possible reaction when using humic acids as catalysts.

Experimental procedure

The ethylbenzene transformation reactions were carried out in a glass continuous down flow fixed bed reactor, at atmospheric pressure. Each experiment was carried out with a 1,5 g of fresh catalyst sample. Before the start of the reaction the catalyst was activated at 200°C for 3 h under nitrogen atmosphere, to drive off the moisture and adsorbed hydrocarbons, if any. The reactants were continuously saturated with nitrogen before being fed into the reactor at the desired temperature, through a HPLC pump. A constant feed flow of 0,05 ml/min was used for all the reactions. The reactions were carried out under atmospheric pressure at temperatures of 180, 250 and 300°C.

3 RESULTS & DISCUSSION

3.1 Introduction

This chapter highlights all the results obtained from the experimental work done. The first results are those on oxidation and the production of humic acids by looking at the different coal types and oxidation methods, for the production of humic acids. Results on the slurry phase oxidation, extraction and characterisation of humic acids as well as results of the test reactions are all presented in this chapter.

3.2 Effect of Coal Type using air oxidation

The extent of oxidation is known to be affected by the temperature as well the time of the oxidation. The same notion applies to the production of humic acids. Regenerated humic acids are also regulated by other parameters such as temperature, and coal rank [31].

3.2.1 Characterization of the feed

Petrographic analysis for determining the rank and the vitrinite content was carried out on the feed. In terms of rank, the coals were found to be typical bituminous coals, medium C rank category. The table below (table 3.1) shows the rank and amount of vitrinites for the coals that were used for the study.

Table 3.1: Petrographic parameters of the coals that were used.

Sample	%RoVmr	Vitrinites (% by volume mineral matter free)	Rank category
Syferfontein	0.61	30.2	medium C
Twistdraai	0.58	36	medium C
Waterberg	0.67	92.4	medium C

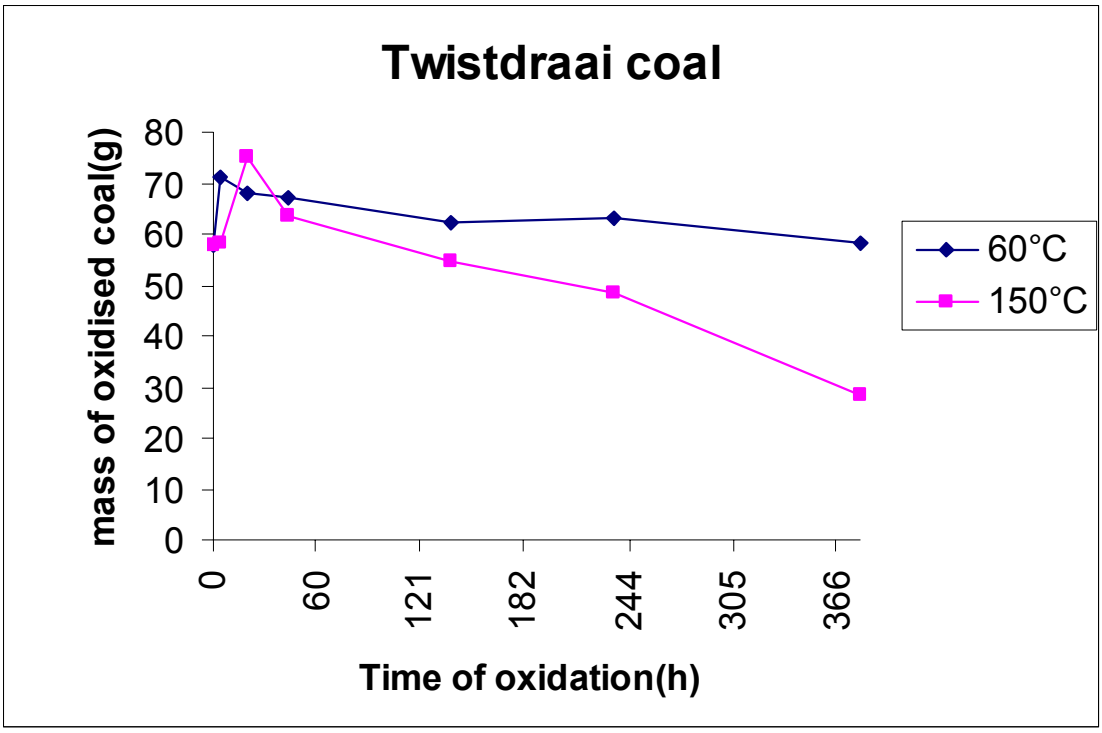
The Twistdraai coal reports the lowest mean random reflectance value (0.58%RoVmr) with Waterberg and Syferfontein reporting 0.67 and 0.61% respectively. Waterberg reports the highest amount of vitrinites content (92.4% by volume). From these results it is noted that Waterberg is high in vitrinite content although all the samples are all of the same rank.

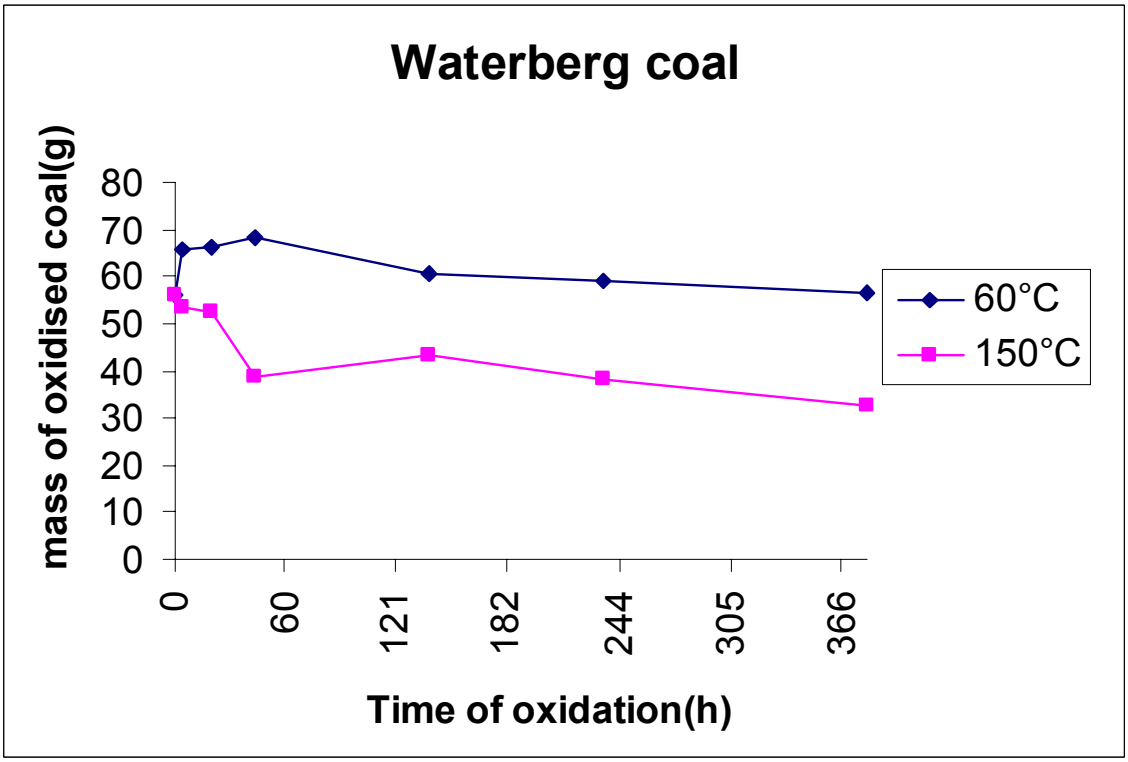
3.2.2 Oxidation product yields

During air oxidation, air is allowed to interact with the surface of the coal, allowing the oxygen in the air to react with the molecular framework of the coal. The oxygen species are incorporated to the coal structure to form carboxylic groups as well as the phenolic groups. The parameters that were varied are the oxidation period with 3, 19, 43, 139, 235, as well as 380 h used, and the reaction temperatures of 60 and 150°C.

Yields of the oxidized coal

The degree of the oxidation of each coal was followed by determining the weight of oxidized product when the reaction was interrupted to take samples. Curves showing these changes in weight are given in figure 3.1. The curves are in agreement with those that were reported by Friedman et al [15].


Twistdraai coal
mass of oxidised coal(g)
80
70
60
50
40
30
20
10
0
0
60
121
182
244
305
366
Time of oxidation(h)
60°C
150°C


Waterberg coal
mass of oxidised coal(g)
80
70
60
50
40
30
20
10
0
0
60
121
182
244
305
366
Time of oxidation(h)
60°C
150°C

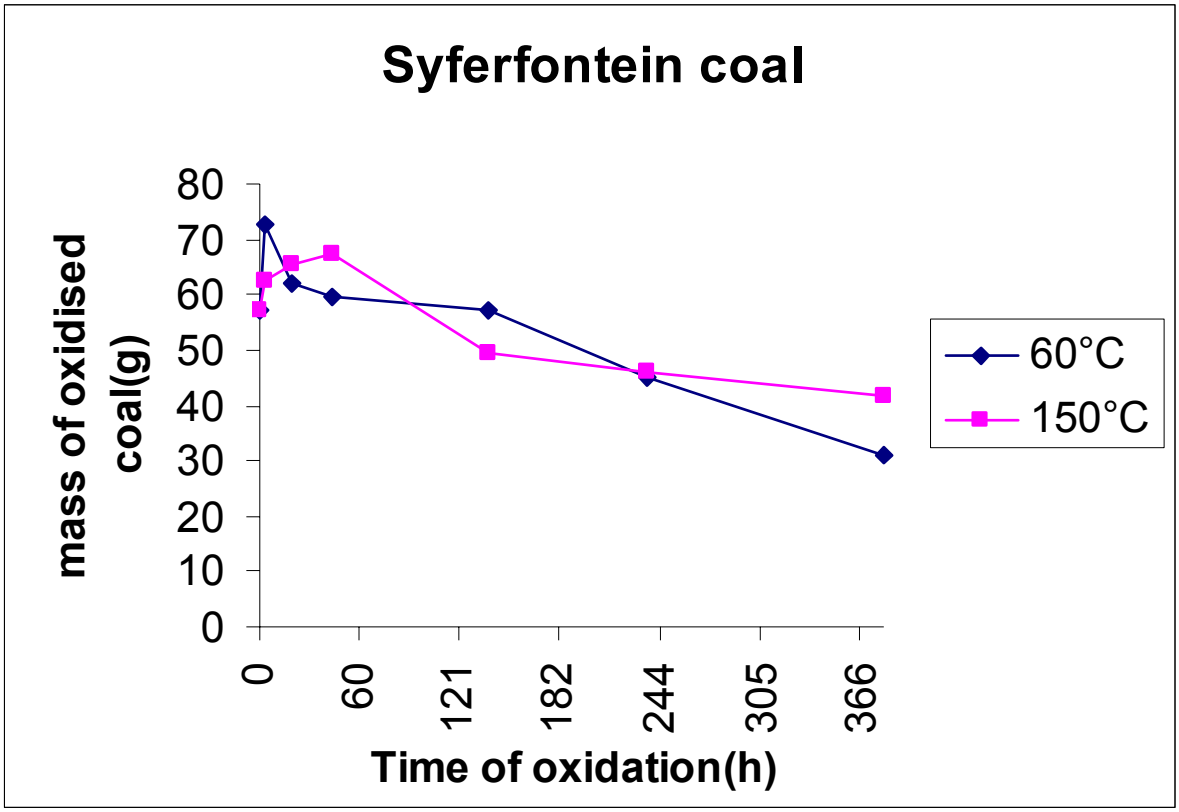


Fig 3.1: The yields of oxidized coal with the extent of oxidation.

It was noted that as soon as the coal is exposed to the oxidizing environment, the mass of the coal tends to increase and then decrease as the reaction proceeds. This can be attributed to the fact that, during the early stages of oxidation, oxygen is incorporated, and this leads to an increase in the mass of the coal. As the oxidation proceeds, CO_2 and CO are released and this leads to a decrease in the yield of oxidized coal. Reactions at 150°C indicate a more notable decrease in the mass with increased reaction times and this indicates the ease of oxidation at elevated temperatures.

Yields of humic acids

Humic acids were extracted from the coals that showed good oxidation. The coals which were used for extraction are Waterberg coal samples oxidised at 150°C, as well as Twistdraai and Syferfontein samples that were oxidized at 150ºC for 379 h as these all showed good oxidation. Table A1 shows the amounts of humic acids extracted for the

Twistdraai, Waterberg and Syferfontein coals all oxidized at 150ºC. Graphical representations of the results obtained from the table A1 are given in figure 3.2 and 3.3. Figure 3.2 shows the effect of reaction time on the yields of humic acids for the Waterberg coal, and the effect of coal type is depicted in figure 3.3.

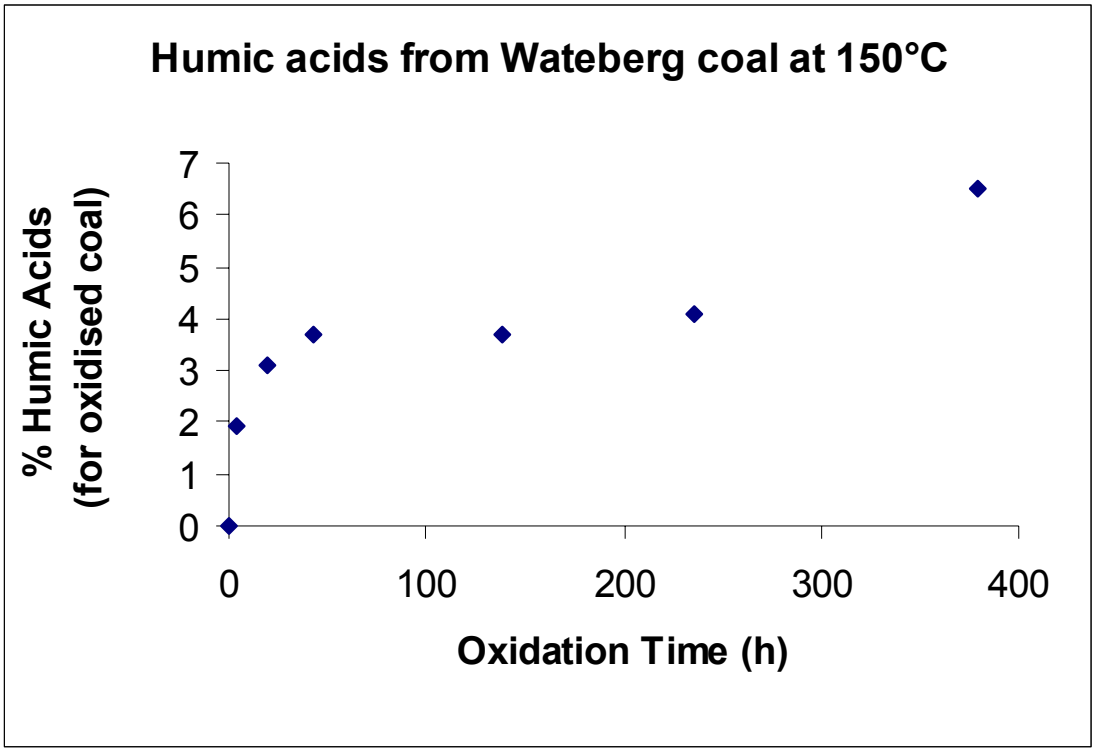


Fig 3.2: Dependence of Humic Acids yields on the reaction time of oxidation

From these results it is apparent that there was an increase in the amount of humic acids as the coal was left to oxidize for longer times. Therefore, the longer the reaction time, the higher the extent of oxidation and thus the higher the yield of regenerated humic acids.

For comparison of the three coals that were used, extraction was carried out from the samples that were oxidized at 150ºC for 379 hours. These were all then compared with each other and the graph below shows the obtained results.

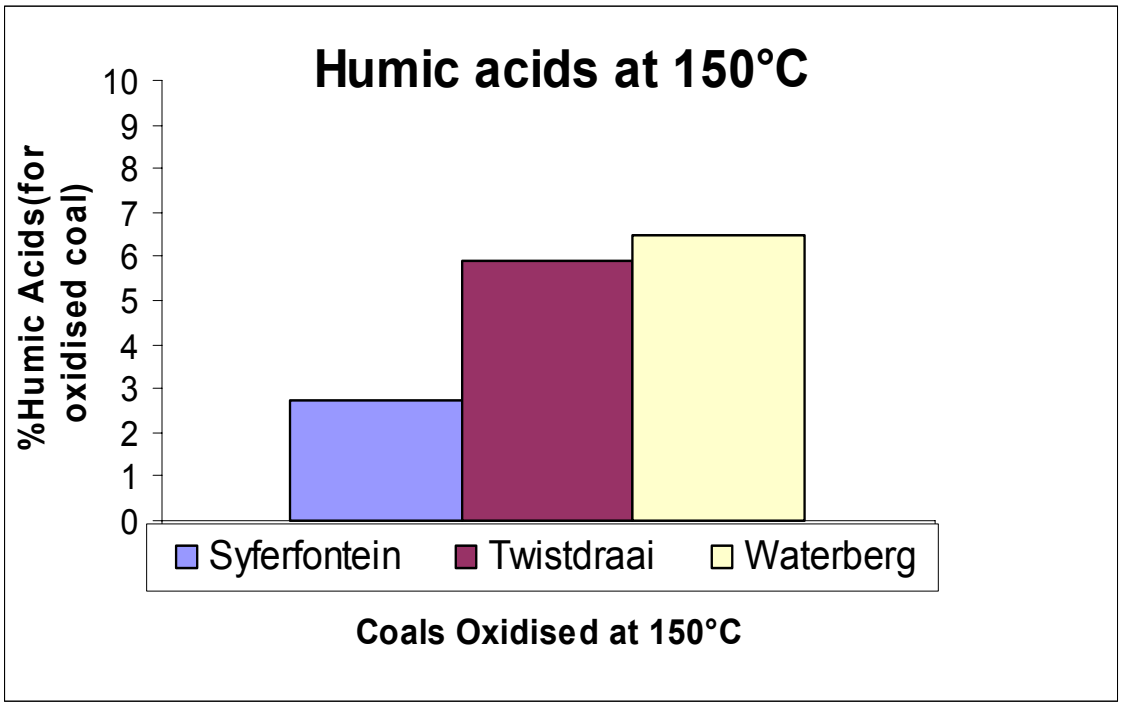


Fig 3.3: Humic acids extracted from the three coals (379h).

The difference shown above can be due to the different characteristics of the coals such as the vitrinite content, amount of carbon that is available to react etc, which affects the reactivity and behaviour of coal.

3.2.3 Characterizations

Ultimate analysis

From the results obtained from ultimate analysis (given in table 3.2-3.4), it can be deduced that Twistdraai and Waterberg coals were more readily oxidised. This is noted from the increase in the oxygen content and the decrease in the C/O ratio, with increasing time of exposure to the oxidizing atmosphere. Syferfontein did not show good oxidation as the oxidation period was increased for both temperatures. With Waterberg and Twistdraai, an increase in temperature of the reaction from 60°C to 150ºC led to an increase in the oxidation reaction. The increase in the oxygen content and the decrease in

the C/O ratio is most pronounced with an increased reaction time, at 150ºC, as compared to that observed at 60ºC.

The better performance of Waterberg coal can be attributed to the fact that it has a high vitrinite content of 92,4%, Twistdraai was found to have 36%, with Syferfontein having 30.2% of vitrinites (obtained from petrographic analysis carried out for the coals used, recorded as % by vol. mineral matter free). Waterberg coal were also found to have a high carbon content, the unoxidized Waterberg coal was found to have a carbon content of 70.91%, while Twistdraai(53.14) and Syferfontein(53.8) have the lowest amounts of carbon content (all recorded as received). Results for ultimate and proximate analysis on the oxidation products are shown in Tables 3.2-3.4.

Table 3.2: Ultimate analysis of Twistdraai coal products

NUMBER	Unoxidized Coal	1	2	3	4	5	6
Reaction Time(h)		3.25	19	43	139	235	379
Twistdraai oxidized at 60ºC							
Proximate analysis							
volatiles	22.32	24.9	25.15	24.66	24.58	24.76	24.54
%ash	29.28	29.96	29.71	29.95	29.74	29.88	29.62
moisture	2.43	1.31	1.24	0.56	0.32	0.33	0.62
Ultimate analysis(a.r)							
%C	53.04	53.12	53.35	52.67	52.70	53.24	53.85
%H	3.16	3.17	3.16	3.30	3.25	3.23	2.94
%N	1.36	1.38	1.38	1.38	1.34	1.32	1.40
%S	0.86	0.88	0.90	0.95	0.89	0.90	0.89
%O	9.87	10.18	10.29	11.19	11.76	11.10	10.25
Twistdraai oxidized at 150ºC							
Proximate analysis							
volatiles	22.32	22.15	23.62	23.27	24.46	24.98	25.88
%ash	29.28	30.3	28.2	31.42	30.73	31.2	29.75
moisture	2.43	0.98	2.15	2.02	1.73	1.89	1.69
Ultimate analysis(a.r)							
%C	53.04	51.48	49.50	48.57	49.14	52.34	48.83
%H	3.16	2.24	1.86	1.77	1.79	2.52	1.75
%N	1.36	1.42	1.44	1.43	1.43	1.30	1.40
%S	0.86	0.88	0.83	0.82	0.86	0.76	0.87
%O	9.87	12.70	16.02	13.97	14.36	17.13	15.71

Table 3.3 Ultimate analysis of Syferfontein coal products

NUMBER	Unoxidized Coal	1	2	3	4	5	6
Reaction Time(h)		3.25	19	43	139	235	379
Syferfontein oxidized at 60ºC							
Proximate analysis							
volatiles	22.92	23.81	24	23.63	23.68	23.7	23.89
%ash	27.95	27.82	27.89	27.92	27.88	27.73	27.67
moisture	2.9	2.27	2.14	2.34	2.16	1.79	1.57
Ultimate analysis (a.r)							
%C	53.80	54.15	54.08	54.35	53.98	54.86	54.89
%H	2.95	2.72	2.70	2.73	2.73	2.67	2.66
%N	1.38	1.36	1.30	1.37	1.34	1.46	1.48
%S	0.68	0.78	0.78	0.79	0.78	0.80	0.78
%O	10.34	10.90	11.11	10.50	11.13	10.69	10.95
Syferfontein oxidized at 150ºC							
Proximate analysis							
volatiles	22.92	24.92	24.48	24.9	25.63	35.2	37.31
%ash	27.95	29.38	30.39	29.83	30.36	30.45	31.04
moisture	2.9	2.75	2.74	2.7	2	1.86	1.55
Ultimate analysis (a.r)							
%C	53.80	51.80	49.37	50.12	50.72	50.12	49.03
%H	2.95	1.92	2.08	1.84	1.91	1.84	1.54
%N	1.38	1.50	1.47	1.49	1.51	1.49	1.57
%S	0.68	0.78	0.74	0.84	0.77	0.84	0.82
%O	10.34	13.83	15.79	14.57	14.62	14.57	14.85

Table 3.4: Ultimate analysis for Waterberg coal products

NUMBER	Unoxidized Coal	1	2	3	4	5	6
Reaction Time(h)		3.25	19	43	139	235	379
Waterberg oxidized at 60ºC							
Proximate analysis							
volatiles	35.47	36.96	35.86	37.55	35.86	36.05	35.99
%ash	9.08	9.95	9.71	10.04	10.12	9.97	9.95
moisture	4.16	1.16	1.72	0.88	0.36	1.18	1.22
Ultimate analysis (a.r)							
%C	70.91	71.99	72.1	71.95	70.46	71.26	70.81
%H	4.66	4.82	4.74	4.81	5.09	4.50	4.39
%N	1.40	1.45	1.43	1.44	1.4	1.46	1.43
%S	1.02	1.06	1.04	1.05	1.04	1.04	1.04
%O	8.77	9.57	9.26	9.83	11.53	10.59	11.16
Waterberg oxidized at 150ºC							
Proximate analysis							
volatiles	35.47	50.25	31.51	28.19	27.07	28.56	29.68
%ash	9.08	15.33	17.42	20.33	22.41	21.53	20.78
moisture	4.16	1.6	0.24	1.48	1.98	1.87	1.9
Ultimate analysis (a.r)							
%C	70.91	67.08	58.18	56.54	55.31	55.23	55.78
%H	4.66	2.43	2.17	1.87	1.48	1.47	1.56
%N	1.40	1.77	1.75	1.99	1.95	2.00	2.04
%S	1.02	0.94	0.84	0.84	0.66	0.91	0.8
%O	8.77	10.85	19.40	16.95	16.21	16.99	17.14

Functional groups determination

Coal comprises molecules containing aromatic rings which undergo substitution reactions of hydrogen with oxygen to form different functional groups during oxidation. The functional groups that are formed are the carboxylic and the phenolic groups. The determination of functional groups was carried out in order to determine the most prefered groups formed during coal oxidation. The relationship between the amount of the specific functional group with the extent of oxidation (increase in oxidation temperature and oxidation period) was studied. Table 3.5 shows the results of the functional groups obtained for all the samples.

Table 3.5: Functional groups obtained from the oxidised products

NUMBER	Unoxidized	1	2	3	4	5	6
Reaction Time(h)	Coal	3.25	19	43	139	235	379
Twistdraai oxidized at 60°C							
functional groups for oxidized coal(meq /g of C)							
carboxylic acids groups	0.06	0.06	0.17	0.18	0.45	0.16	0.13
phenolic groups	5.90	6.86	4.87	5.68	6.86	6.94	6.67
total acids groups	5.96	6.92	5.04	5.86	7.31	7.10	6.80
Twistdraai oxidized at 150°C							
carboxylic acids groups	0.06	0.09	0.16	0.37	0.57	0.68	1.18
phenolic groups	5.90	6.22	7.25	9.11	11.35	11.70	12.03
total acids groups	5.96	6.31	7.41	9.48	11.92	12.38	13.21

Syferfontein oxidized at 60°C							
carboxylic acids groups	0.07	0.12	0.11	0.15	0.17	0.17	0.16
phenolic groups	5.62	5.87	5.82	6.76	6.04	6.30	4.81
total acids groups	5.69	5.99	5.93	6.90	6.21	6.47	4.97
Syferfontein oxidized at 150°C							
carboxylic acids groups	0.07	0.19	0.30	0.54	0.52	0.64	0.67
phenolic groups	5.62	6.63	6.45	13.30	9.19	9.68	12.20
total acids groups	5.69	6.82	6.75	13.84	9.71	10.32	12.87
Waterberg oxidized at 60°C							
carboxylic acids groups	0.06	0.13	0.13	0.02	0.04	0.05	0.10
phenolic groups	4.92	6.47	6.59	4.94	5.53	5.55	5.88
total acids groups	4.98	6.60	6.72	4.96	5.57	2.20	3.00
Waterberg oxidized at 150°C							
carboxylic acids groups	0.06	0.13	0.73	0.96	0.98	1.21	1.22
phenolic groups	4.92	6.41	11.63	11.88	6.80	10.50	12.11
total acids groups	4.98	6.54	12.36	12.84	7.78	11.71	13.33

The results of the functional groups content were plotted to establish trends that are associated with different reaction conditions employed, these are presented in the following section.

Carboxylic acid groups

The results obtained for these functional groups are given for each coal type at the two oxidation temperatures, i.e. 60°C and 150ºC. Figure 3.4 shows the graphical representation of the results obtained for the behaviour of carboxylic acids with increase time of oxidation for the samples oxidised at 60 °C.

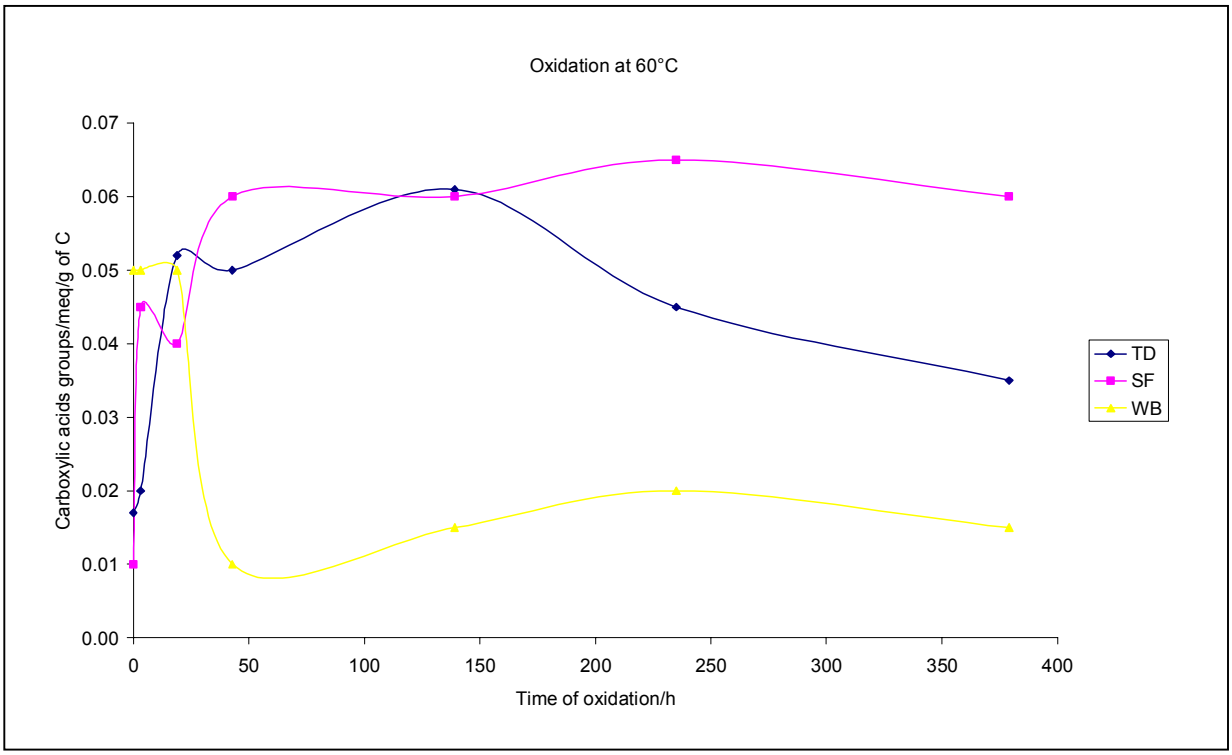


Fig 3.4: The amount carboxylic groups for the Waterberg (WB), Syferfontein (SF) and Twistdraai (TD) coals oxidized at 60ºC.

From these results it is noted that for all the coals there were no significant changes as the reaction progressed. This indicated that with oxidation of coal at 60ºC, the amounts of carboxylic acids are not affected notably, with the variation being between 0.01 to 0.06 meq/g of C for 379 h. Figure 3.5 indicates the behaviour of the carboxylic acids with increase in reaction time at 150°C for the samples used.

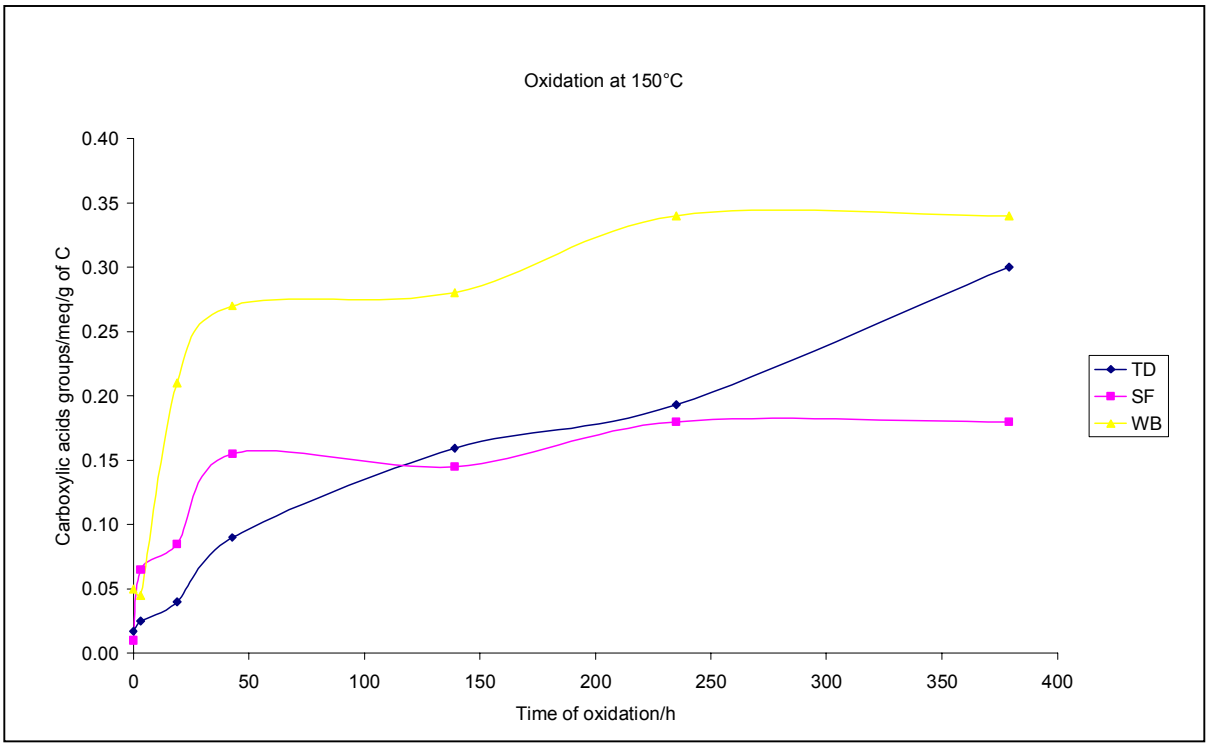


Fig 3.5: The amount carboxylic groups for the Waterberg (WB), Syferfontein (SF) and Twistdraai (TD) coals oxidized at 150ºC.

A notable increase (compared to reactions at 60°C) in the amount of carboxylic acids was obtained with the oxidation at 150°C. For all three coals used, there was an increase in the amount of carboxylic acids with increased reaction extent. Waterberg showed a greater increase of carboxylic acids, compared to the other coals, with Twistdraai also showing good content of carboxylic acids with increased reaction extent. From the graphs given it is noted that the higher formation of the carboxylic acids is obtained with the oxidation at 150ºC, for all the coals. It can be concluded that the yields of the carboxylic acids increase with an increase in temperature, as expected.

At high temperatures (150°C) Waterberg tends to react to form carboxylic acids as soon as it is exposed to the oxidizing environment; this is deduced from the fact that there was a sharp increase in the amount of carboxylic acids within the first 100 hours of the reaction. Twistdraai also showed a good formation of the carboxylic acids, but the

increase was not as sharp as it was with the Waterberg coal. Syferfontein showed the lowest amount of carboxylic acids formed during oxidation.

Phenolic groups

The phenolic groups were measured using the difference of carboxylic acids and total acids as explained earlier. After the phenolic groups were determined, the results for all the oxidized coal samples were compared for the three coals that were used at 60ºC and 150ºC. Figure 3.6 and 3.7 shows the results given in table 3.2-3.5 obtained with oxidation at 60 °C and 150°C respectively.

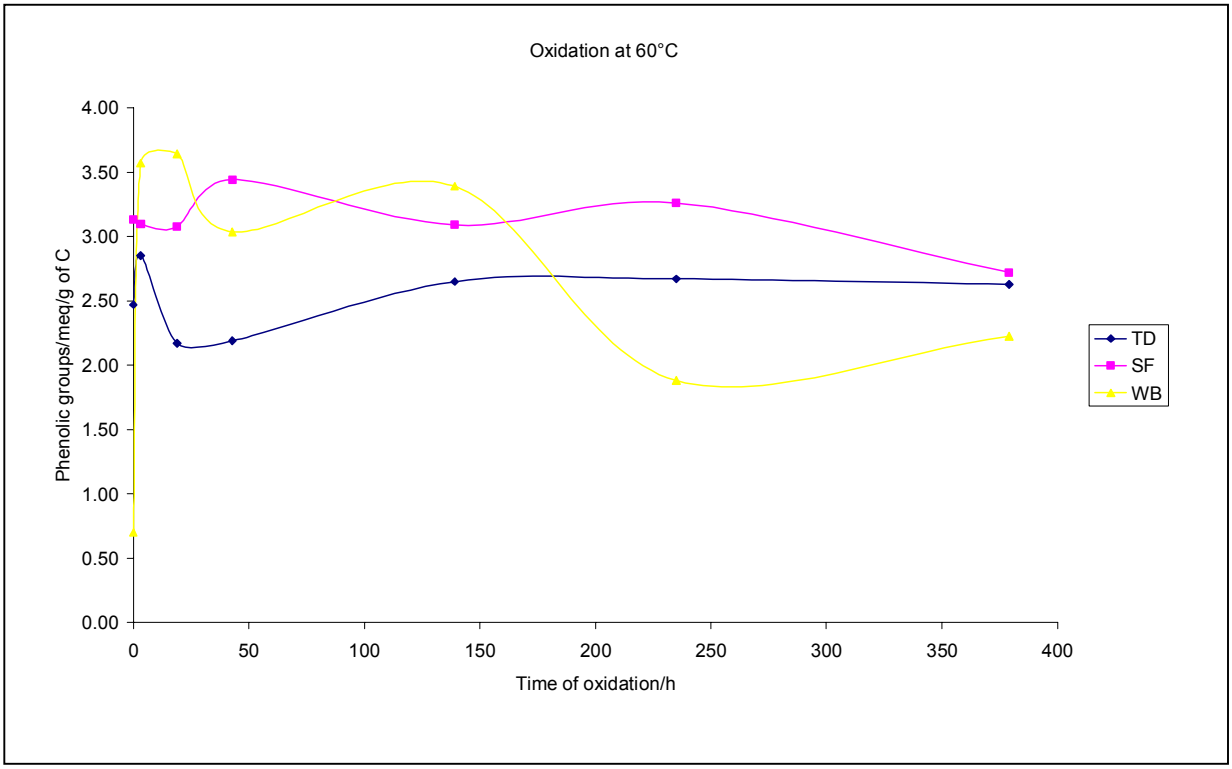


Fig 3.6: The amount of phenolic groups for the Waterberg (WB), Syferfontein (SF) and Twistdraai (TD) coals oxidized at 60ºC.

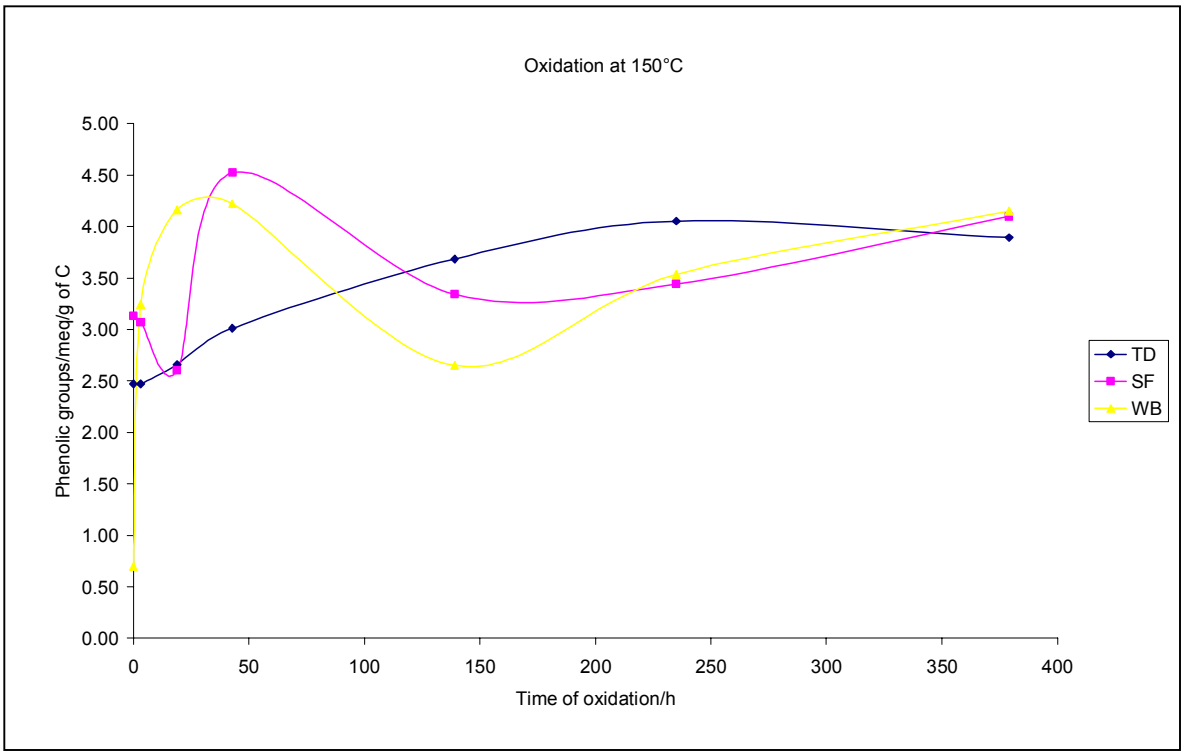


Fig 3.7: The amount of phenolic groups for the Waterberg (WB), Syferfontein (SF) and Twistdraai (TD) coals oxidized at 150ºC.

A slight increase in the amount of phenolic groups is noted for the three coals at 150°C. This slight increase can be due to the fact that there was a corresponding increase in the amount of carboxylic acids with temperature. The increase in the amount of phenolic groups is minor as compared to that of carboxylic acids. This showed that oxidation and optimisation of reaction conditions favoured the formation of carboxylic acids.

IR analysis on Waterberg oxidation products

IR analysis was carried out on the Waterberg coal products i.e. the unoxidised coal, the oxidised coal and the humic acids extracted from the Waterberg coal. The spectra obtained are shown in figure 3.8.

From the results shown in the spectra, a strong absorption around 3000cm^{-1} is indicative of the –OH stretch of the carboxylic acid as well as OH of the hydroxyl groups. The

absorption around 1706 cm^{-1} shows the presence of the C=O of the carboxylic acids. There was an increase in intensity of these two peaks (OH and C=O) from coal to oxidised coal and from oxidised coal to humic acid. This indicated an increase in the amount of these functional groups due to oxidation, and the extraction of humic acids.

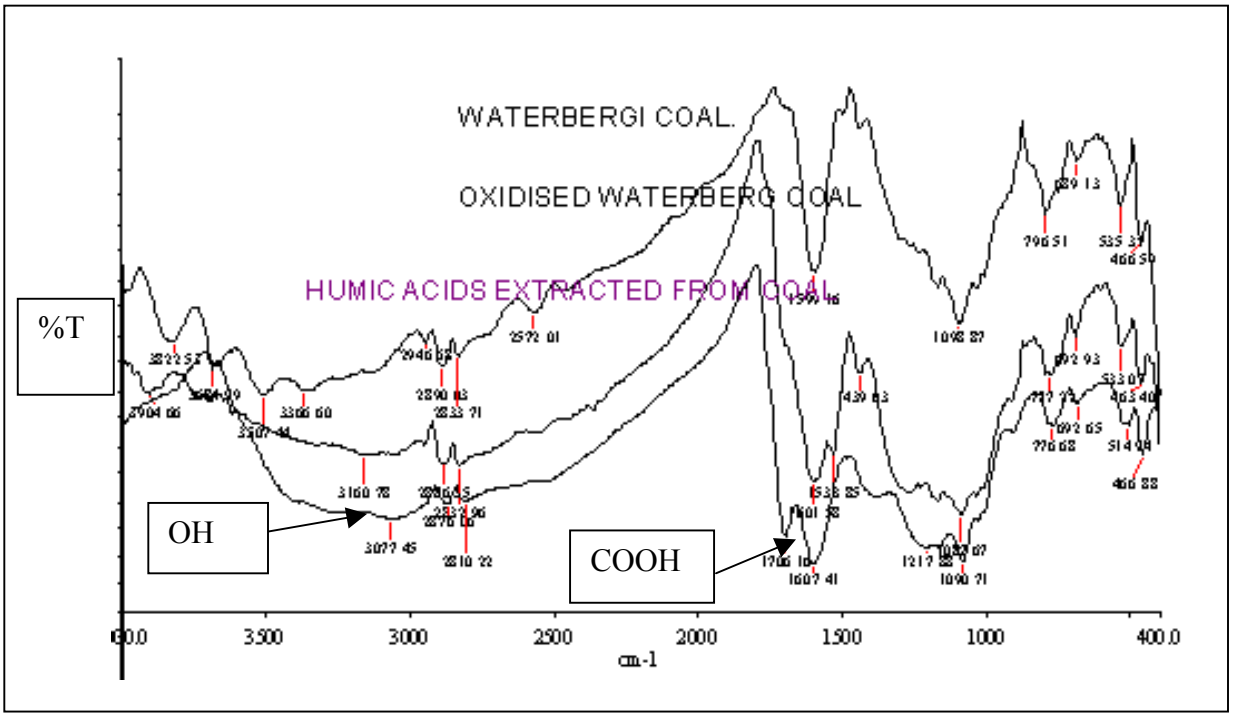


Fig 3.8: FT-IR spectra of the Waterberg oxidation products

The major functional groups in oxidised coal and humic acids are carboxylic and phenolic groups. The most important absorptions are recognizable in the "carbonyl" region (1690-1800 cm^{-1}) and in the zone where single C-O bonds absorb (1290-1000 cm^{-1}). The most important functional groups are carboxylic and phenolic groups which are responsible for the behaviour and performances of these substances in solution.

3.2.4 Conclusions

No coal oxidation at 60°C was observed with air as an oxidant. Slight oxidation can be accomplished using air oxidation at elevated temperatures (in this case 150°C). This was

deduced from the increased amount of oxygen in oxidized coals with increased oxidation period, as well as from the increase in amount of carboxylic acids and phenolic groups.

Waterberg coal was found to be the easiest to oxidize and it produced higher amounts of carboxylic acids than did Twistdraai and Syferfontein coals. Twistdraai showed better incorporation of oxygen and a notable increase in carboxylic acids and phenolic groups. Syferfontein was not easily oxidized even at 150°C.

Humic acids were successfully extracted and characterized. The yields were found to increase with increasing oxidation periods and reaction temperatures. Waterberg gave the highest yield of humic acids compared to Twistdraai and Syferfontein under the same oxidation conditions (150°C for 380 h). Twistdraai gave the second highest yield while Syferfontein gave the lowest yield of humic acids.

It can also be concluded that the extent of oxidation and humic acids yield do depend on the rank and the amount of vitrinites in the coal. Waterberg which had the highest amount of vitrinites showed good oxidation and highest humic acids yield. Twistdraai which was the lowest ranked coal of the three also showed good oxidation and production of humic acids.

3.3 Slurry phase oxidation

Due to low yields in the oxidation reactions using air oxidation, a more robust oxidation method was employed in order to improve the extent of the reactions and also the yields of humic acids. Slurry phase oxidation was employed since the reactions can be carried out under elevated temperatures of up to 200°C and high pressures up to 80 bars.

Waterberg coal was the only coal used for this investigation as it was shown in the previous chapter that due to their high vitrinite content Waterberg sample seemed to perform better than the other coal types. The reactions were carried out at different temperatures of 120, 140, 160, 180, and 200°C, under a constant pressure of 40 bars.

3.3.1 Oxidation product yields

The degree of oxidation of each coal was followed by determining the weight of oxidized product after each reaction. The mass of fulvic acids produced was also determined. Table A2 shows the results obtained with oxidation at different conditions. The table show yields of oxidized coal together with elemental compositions reported as received. The yields of the humic acids and fulvic acids are also indicated.

During oxidation reaction carbon dioxide and carbon monoxide are released as by-products. The amount of these by-products is calculates as:

$$\%C_{(CO2+CO)} = \%C \text{ coal} - \%C_{\text{oxicoal}} - \%C_{\text{fulvic acid}}$$

From the results in the table A2 it is noted that the mass of the oxidized coal (based on carbon) decreases with the increased extent of oxidation (graph figure 3.9). This was expected as mentioned in section 3.2.2.

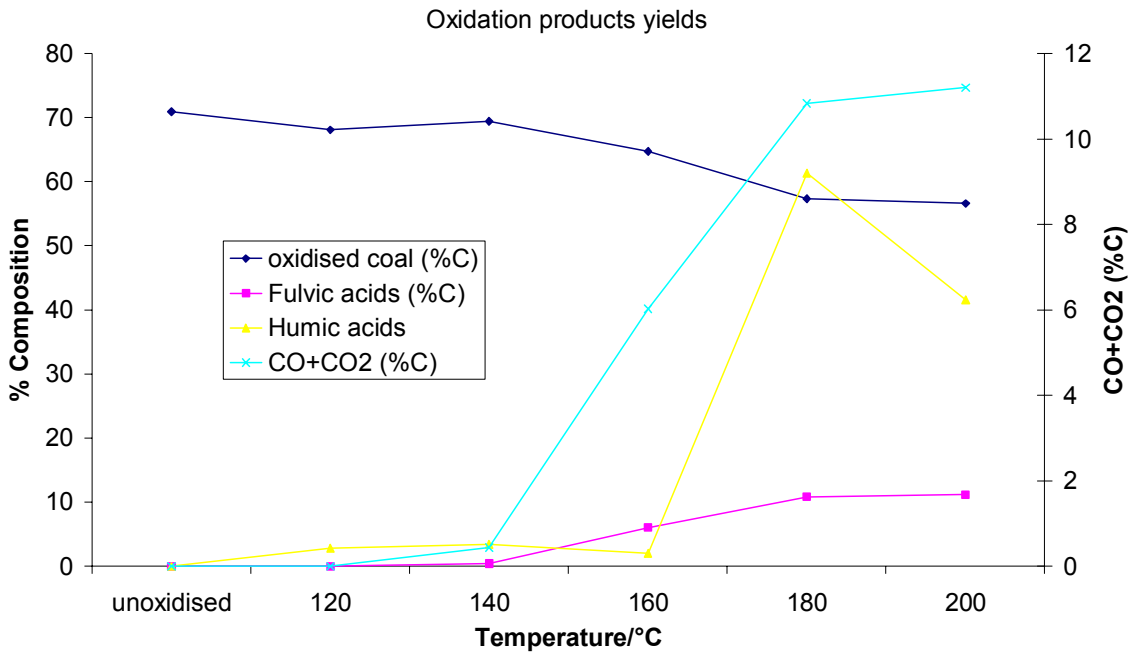


Figure 3.9: Oxidation products yields for Waterberg coal slurry phase oxidation

At lower oxidation temperatures oxygen was incorporated and this led to an increase in the mass of coal. As the oxidation temperatures were increased CO_2 and CO were released and this led to a decrease in the yield of oxidized products. The percentage carbon of the oxidized coal also decreased with increased oxidation temperatures. This can be attributed to the observed loss of more CO and CO_2 with increased reaction temperatures.

The yield of humic acids was also found to increase with the reaction temperatures, under the slurry phase oxidation conditions. This can be attributed to the increasing ease of reactivity with the increased temperatures which also leads to the formation of more humic acids. The amount of humic acids was found to be optimum at 180°C and a decrease was observed with oxidation at 200°C. This can be due to a large amount of CO and CO_2 that was lost at 200°C.

Fulvic acids were produced in very low amounts; however there was an increase in the amount of fulvic acids formed with an increase in reaction temperatures. This was also attributed to an increase in the extent of oxidation with temperatures.

3.3.2 Characterizations

Ultimate analysis

From the results obtained from ultimate analysis (given in Table A2), it can be deduced that there was a noticeable increase of oxygen with the increased reaction temperatures. A decrease in the amount of carbon with increasing reaction temperatures was also observed. This was indicative of the increased extent of oxidation with increased reaction temperature.

Functional groups determination

Coal consists mainly of aromatic rings which undergo substitution reactions of the hydrogen with oxygen to form different functional groups during oxidation. The functional groups that were formed are the carboxylic acid groups and the phenolic groups. The determination of functional groups was carried out in order to determine the most favourable groups that were formed during the slurry phase oxidation. The relationship between the amounts of the specific functional groups with the extent of oxidation (increase in oxidation temperatures) was studied. Table A3 shows the amounts of functional groups obtained at different temperatures.

The results in table 3A indicated an increase in the amount of carboxylic acids as the temperature of the reaction is increased. The amount of carboxylic acids given as mille equivalence per gram of carbon was low in the unoxidized coal; however, a gradual increase was noted with the increasing temperatures. This is shown graphically in figure 3.10.

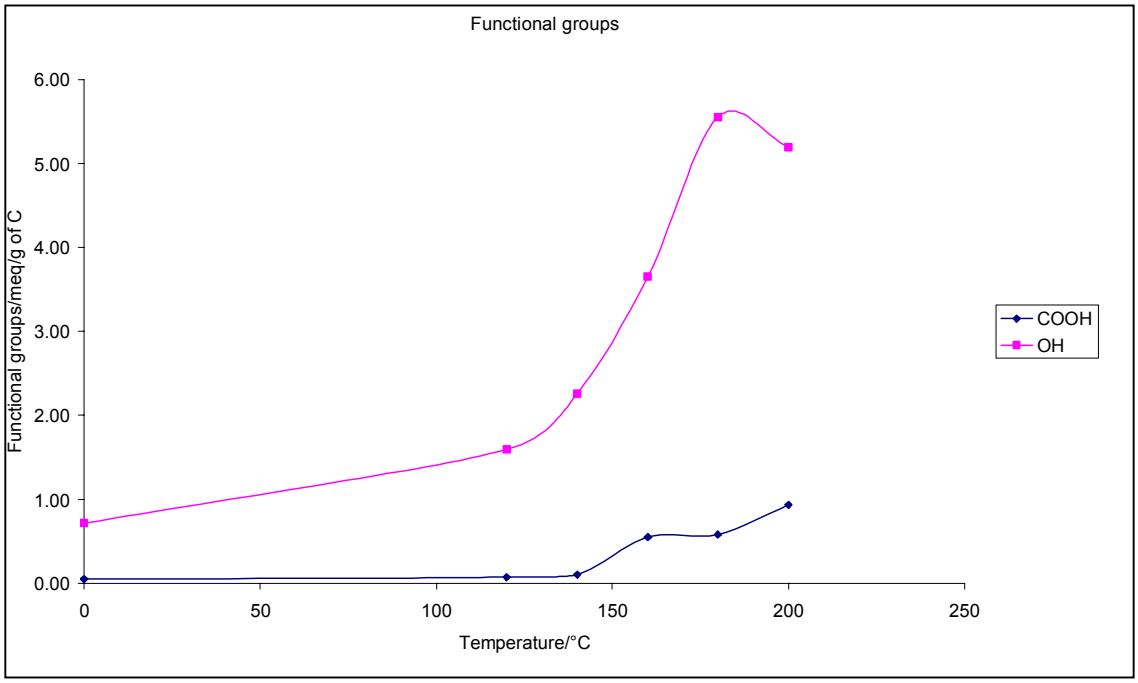


Fig 3.10: The behaviour of functional groups with increased temperatures of the reactions.

The amounts of phenolic groups also show an increase as the temperature is increased. It is noted however that the amount of phenolic groups is higher than that of the carboxylic acids, even with the unoxidized coal. The ratio of phenolic groups to carboxylic acid groups shows that there is an increase of carboxylic acids with increased temperatures. This is seen from the fact that the ratio (phenolic/carboxylic) approaches a unit from high values as the temperature increase (table A3).

3.3.3 Conclusions

The extent of oxidation using slurry phase oxidation in an autoclave was dependant on temperature of the reaction. The increase in oxygen content and a decrease in carbon content with increased reaction temperatures indicated an increase in the extent of oxidation. This was also illustrated by the increase in the amount of $CO + CO_2$ that was formed at higher temperatures. The distribution of functional groups was also found to be dependant on the reaction temperature. There was an increase in both phenolic and carboxylic acid groups with increased temperature.

3.4 Acid catalysis characterizations on humic acids and zeolites

3.4.1 Strength and type of acid sites

The determination of the acidity of mordernite, Y-zeolite and humic acids was carried out using FTIR. However, humic acid was difficult to analyze with transmission FTIR since it was not IR transparent. A recommendation was made to study humic acid with the DRIFTS at Wits University. Figure 3.11 shows an FTIR spectrum of both the mordenite and Y-zeolites for the determination of the type of acid sites.

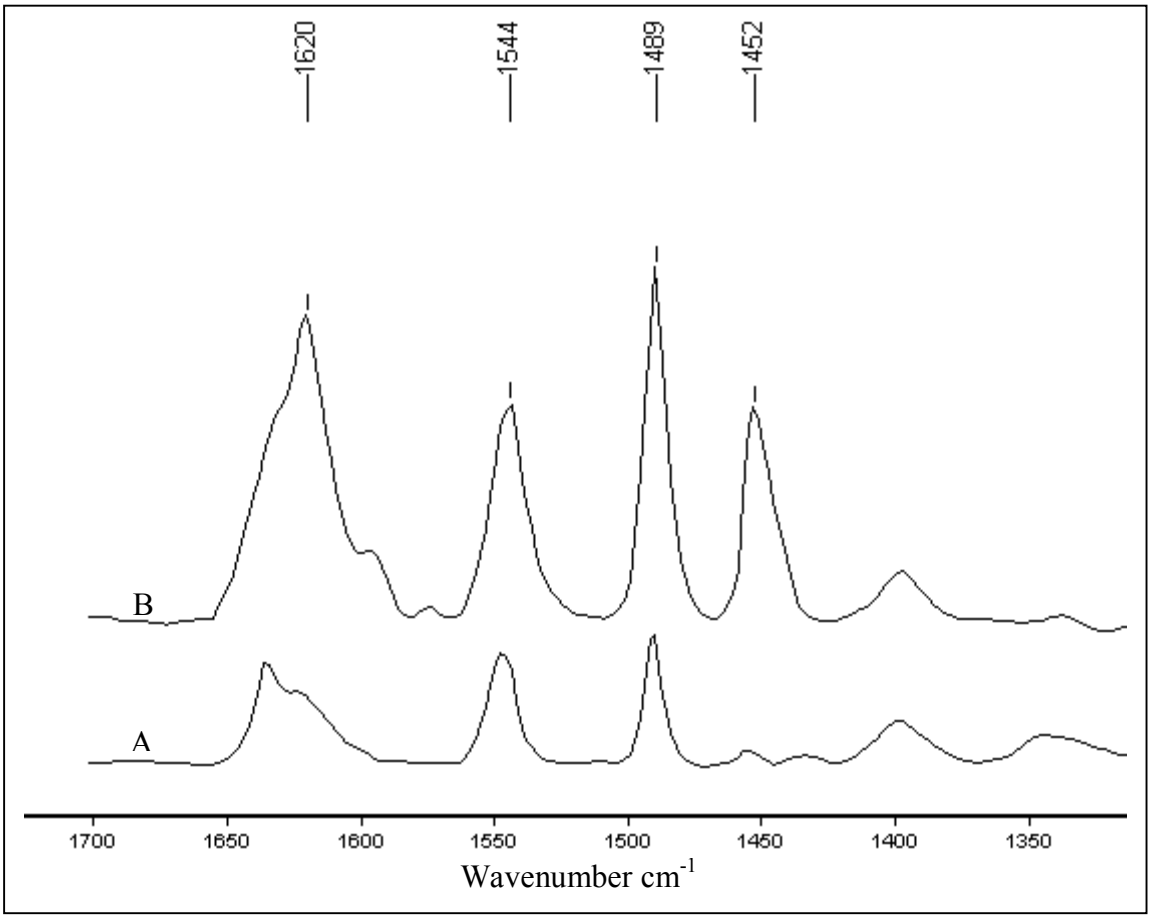


Figure 3.11: FTIR spectra of (A) H-Mordenite (B) H-Y Zeolite after pyridine adsorption

These results show that both samples have Brønsted (1544 cm^{-1}) and Lewis (1452 cm^{-1}) acid sites. H-Y zeolite has more Lewis and Brønsted acid site than H- Mordenite. H-Mordenite contains predominantly Brønsted acid sites and considerably less Lewis acid sites. It was observed that in both zeolites the Brønsted acid sites are more than the Lewis acid sites (Table A4). The strength of the Lewis acid sites in both the samples is the same. This is so because the Lewis acid sites peak in the two samples appears at the same wavenumber. If there was a difference in the strength of the Lewis acid sites, this would be indicted by the shift in the peak to higher wavenumbers. The position of the peaks is in agreement with the results reported by Khabtou et al [46].

The spectra region showing the hydroxyl groups present in zeolites is presented in Figure 3.12. In both spectra the negative peaks in the 3600 – 3700 cm^{-1} range are of the hydroxyl

groups prior to pyridine adsorption. The peak at ca. 3745 cm^{-1} is due to the terminal silanol group. In H-Mordenite, two peaks at 3650 cm^{-1} and 3570 cm^{-1} were observed. These peaks can be associated with the structural high frequency (HF) and low frequency (LF) hydroxyl groups respectively. The intensities of the peaks suggested that the (HF) OH groups were dominant. (HF) OH groups are commonly found in the supercages while the LF OH groups are found in small cages.

In H-Y zeolite, there were more than two peaks in the 3550 – 3570 cm^{-1} region. This is an indication of the presence of other hydroxyl groups other than the (HF) OH and (LF) OH groups. These extra hydroxyl groups can be attributed to the hydroxyl groups on the extra framework alumina atoms. This result suggests that some dealumination occurred in H-Y zeolite thus the presence of extra framework aluminium species. After pyridine adsorption the hydroxyl peaks shifted to the 3100 cm^{-1} region.

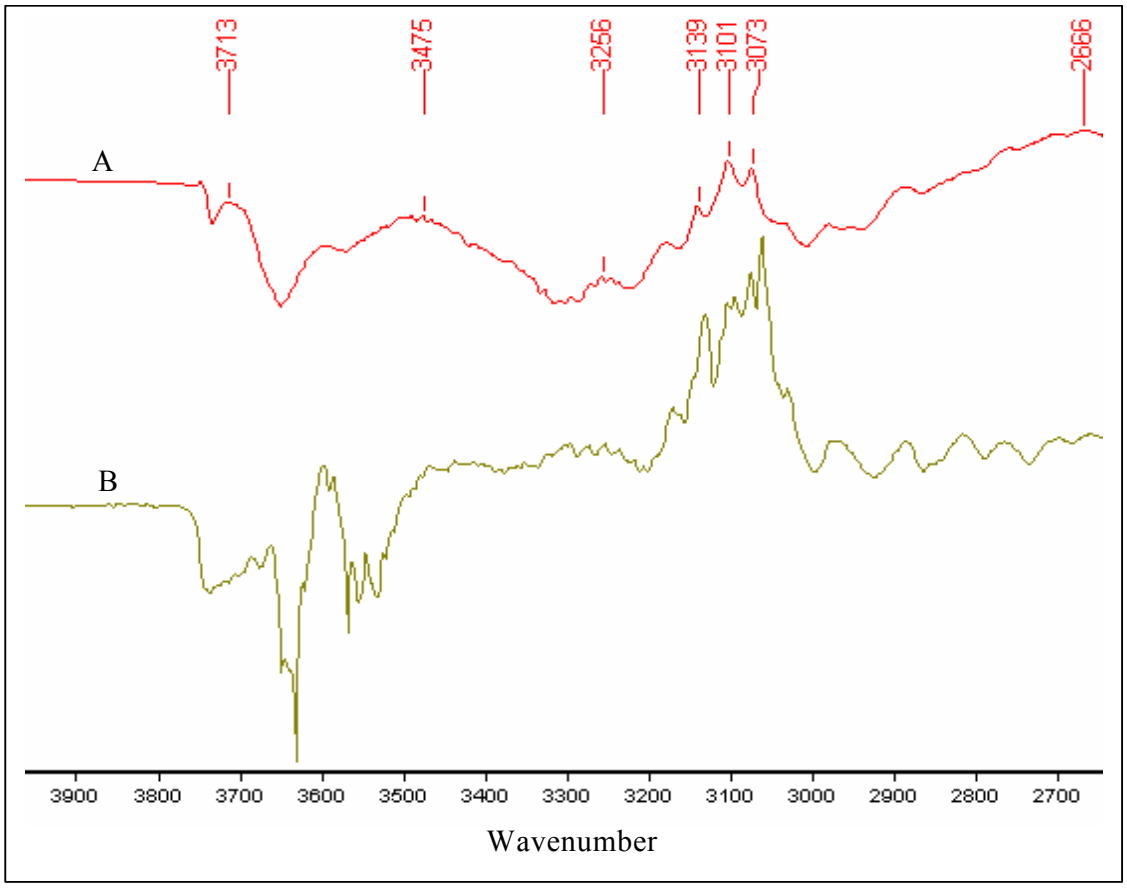


Fig. 3.12: FTIR spectra of (A) H-Mordenite (B)H-Y Zeolite in the Hydroxyl region

Due to the fact that humic acids were not IR transparent, DRIFTS was used to analyse humic acids samples, on KBr pellets. From this investigation it was proven that the structure of humic acids is so complicated such that it is difficult to study acidity using spectroscopic techniques. Figure 3.13 shows the spectra (1350-1700cm^{-1} region) obtained for humic acids characterisation. From the spectrum it was noted that it was difficult to quantify the acidity of humic acids using IR techniques due to interference of their functional groups.

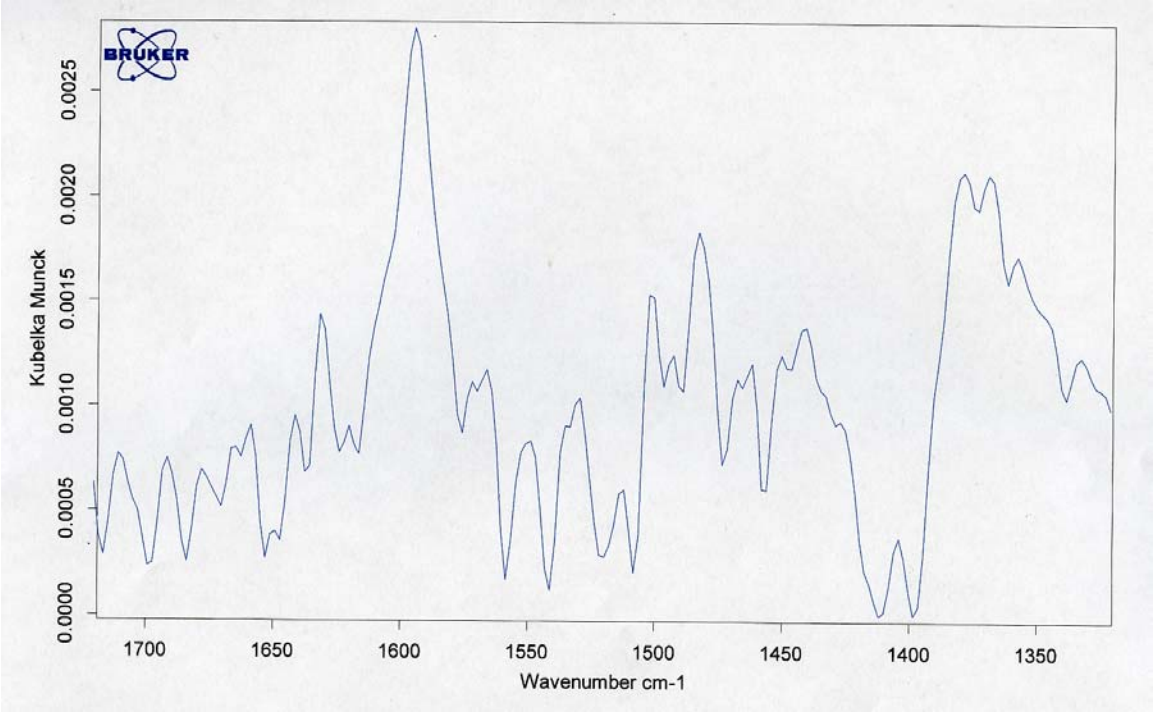


Fig 3.13: DRIFTS spectra of humic acids

3.4.2 Amount/concentration of acid sites

The acidity of the extracted humic acids was also determined by measuring the amount of H^+ ions per gram of dry resin, the results were compared to those of zeolites chosen for this study. The results are given in figure 3.14.

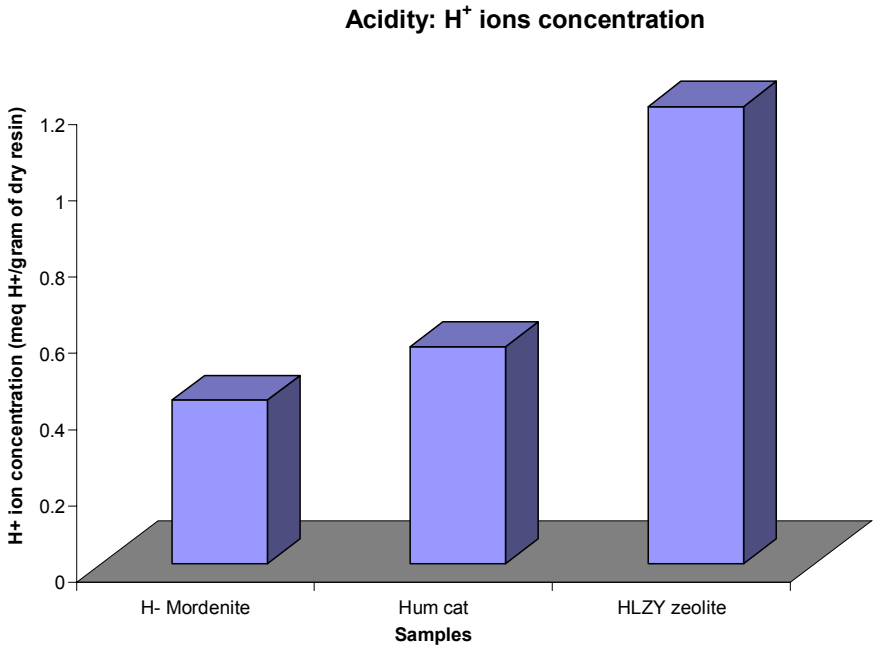


Figure 3.14: Amount of active sites per gram of dry resin

From these results it is noted that the acid density of humic acids referred to as hum cat (0.57 meq H^+ ions/gram of dry resin) is larger than that of mordenite (0.43 meq H^+ ions/gram of dry resin), but it's less than that of Y zeolite (1.2 meq H^+ ions/gram of dry resin). This indicates that the concentration of H^+ ions of the humic acids is comparable with those of zeolites. Since the method used involved titration with a base, the observed acidity on humic acids might be due to the fact that the method will analyse for all the protons that are on the structure including those that cannot take part in catalysing reactions. The differences between zeolites is mainly due to structural differences, the three dimensional structure of the Y-zeolite offers extensive excess to active sites. It is well known that mordenite contains stronger sites than zeolite Y although the later has a higher density.

3.4.3 Thermal analysis

Thermo gravimetric analysis (TGA)

The results obtained from the TGA of the three samples (fig. 3.15) show that the two zeolites exhibited good thermal stabilities as there was no loss in mass up to 900°C even with the change of atmosphere from inert to an oxidizing atmosphere. In the case of humic acids a loss in mass is noted with an increase in temperature under inert atmosphere. This is probably due to liberation of volatiles and/or the breaking down of functional groups analogous to thermal cracking.

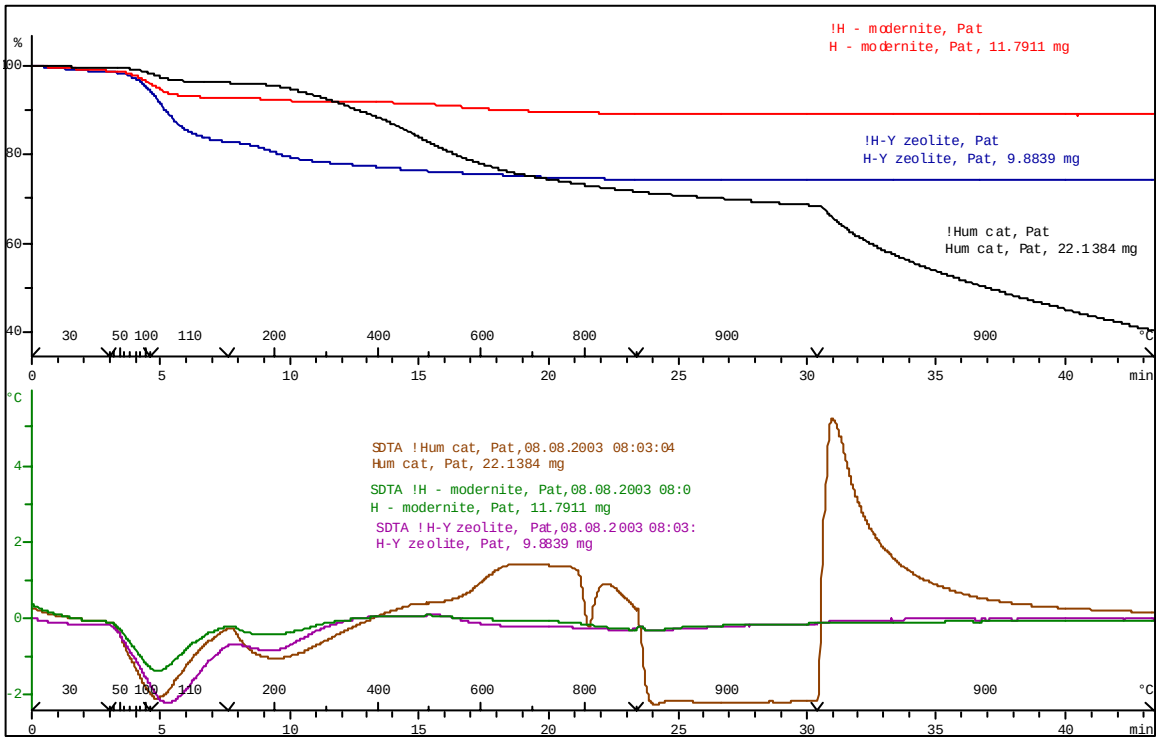


Figure 3.15: TGA plot of the samples

Detailed thermal analysis of humic acids

Detailed thermal analysis study on humic acids was carried out in order to determine the species lost at different temperatures. The TGA plot obtained for humic acids extracted from Waterberg coal oxidised at 180°C is shown in figure 3.15. From the plot it is illustrated that a loss in mass was experienced with increase in temperature. The TGA plot shows an initial loss of mass at about 100°C which was probably due to loss of free moisture. No further loss in mass was observed up to about 300°C. A gradual decrease in mass was observed between 300 and 800°C under N_2 atmosphere. An oxidising atmosphere was employed at 800°C and higher temperatures where a further loss of mass was observed.

Humic acids were subjected to thermal treatment for an hour's period at 200, 400, 600, 800, and 1000°C under N_2 atmosphere. After each run the samples were quenched under N_2 and weighed. The effects of thermal treatment on the mass are depicted in figure 3.16.

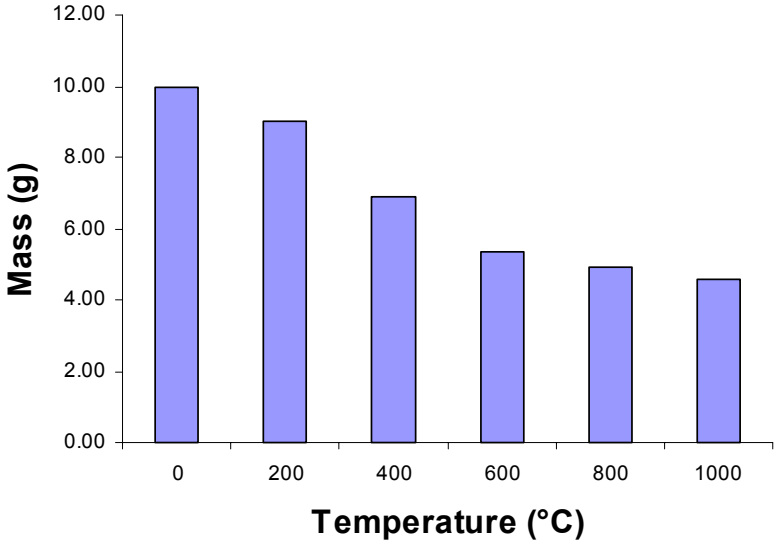


Figure 3.16: Mass loss experienced with thermal treatment of humic acids
(Note: 0 temperature denote room temperature)

The observed mass loss is in agreement with the results obtained with the TGA. From the graph, a notable change in mass was experienced at 400°C. This is in agreement with the observations from the work reported by Lu et al [43] and Mangrich et al [44] that the humic acids are stable to about 300°C. The decrease in mass for the sample at 200°C was caused by the loss in the free moisture on the humic acids.

The impact of thermal treatment on the acidity (phenolic and carboxylic acids) was monitored. Figure 3.17 depicts the impact of thermal treatment on the distribution of the carboxylic acids, phenolic acids as well as the total acids. The functional groups are reported as the milli-equivalence (meq) per gram of carbon.

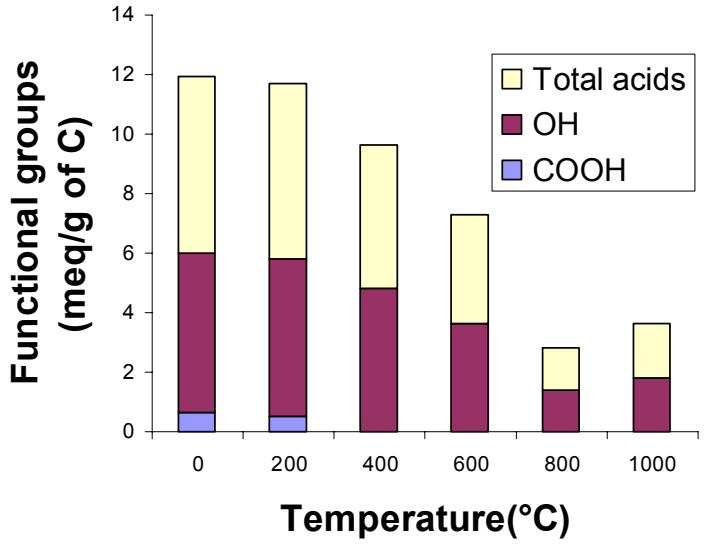


Figure 3.17: Functional groups on the humic acids after thermal treatment

It is observed from the given results that there was a decrease in the number of total acids with increase in temperatures. However the decrease was experienced at temperatures above 200°C. Of the acidic functional groups (i.e. carboxylic and phenolic acid groups), carboxylic acids seem to be the least stable and are lost at low temperatures with none detected at 400°C. This was due to decarboxylation reactions that take place at the temperatures where carboxylic acids are lost. Phenolic acid groups were found to be more stable although they were also lost at more elevated temperatures (400°C to 600°C). The

FTIR spectra of humic acids recorded at the temperatures mentioned are shown in figure 3.18.

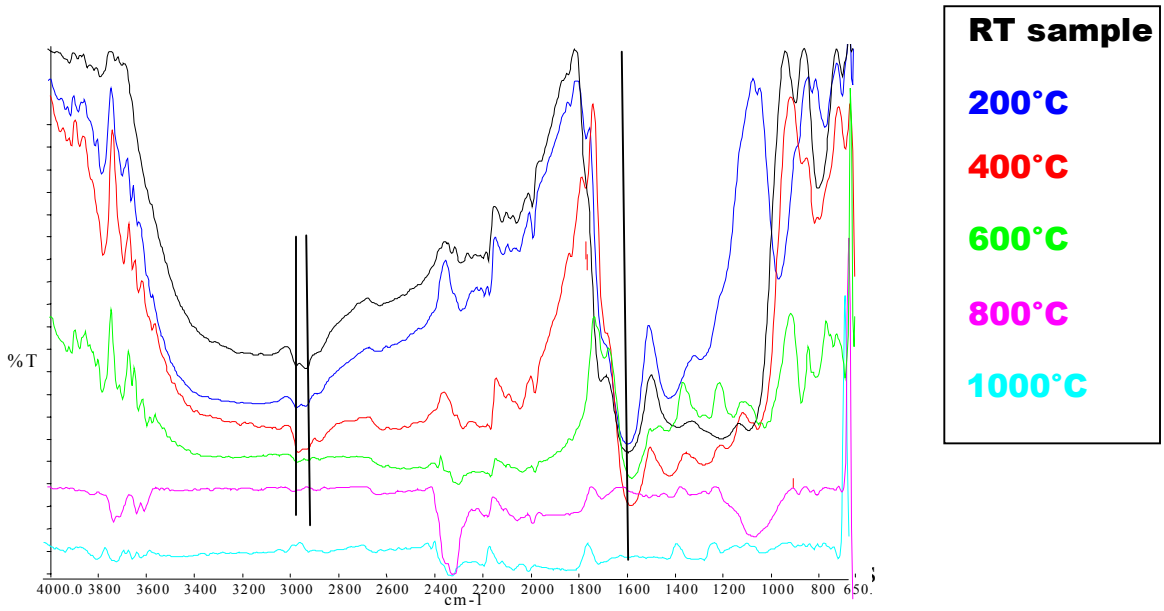


Fig 3.18: IR spectra of the thermally treated humic acid samples

There is not much difference in the spectra for humic acids before thermal treatment and the humic acids treated at 200°C. This was in agreement with TGA and DTA results which indicated that the mass loss was due to the loss of free moisture which will have no effect on the chemical structure. A rapid reduction in the intensity of the COOH band at 1400-1600cm^{-1} became more pronounced with increasing temperature to 400°C and 600°C; at 800°C the COOH band was no longer detected. This is in agreement with the results obtained with the functional groups determination which showed a rapid loss of the carboxylic acids groups with increase in temperature.

The conversion of the aliphatic C-H band in the 2800-3000 cm^{-1} region to the aromatic C-H band in the 3000-3100 cm^{-1} region at temperatures between 200 and 600°C is also shown in figure 3.18. On increasing the temperature from 200 to 600°C, there was a gradual loss in the bands from aliphatic C-H and an increase in aromatic C-H intensity which remain up to 600°C. This was in agreement with the findings of the work by Lu et al [43].

The comparison of the carbon to hydrogen (C/H) shown in figure 3.19 also showed that there was an increase in the C/H ratio with increase in temperature, which suggest an increase in aromaticity.

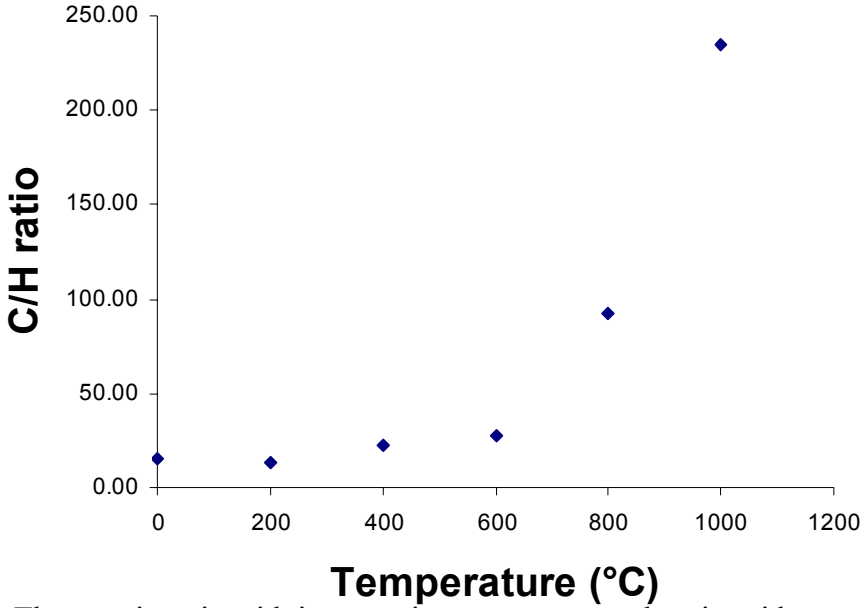


Fig 3.19: The atomic ratio with increase in temperature on humic acids.

An increase in the C/H ratio was observed with increase in temperature and a sharp increase was observed above 600°C, this was probably due to the loss of hydrogen that reacts with the oxygen on the structure and is liberated as H_2O at elevated temperatures. This was illustrated during pyrolysis of different coal types by Arenillas et al [46]. The decrease in hydrogen gives rise to an increase in C/H which suggests a formation of substance of high aromaticity.

These results were consistent with the observations obtained with the IR analysis. It was observed that below 600°C a switch from aliphatic C-H to an aromatic C-H was taking place. This means an increase in aromaticity, which was consistent with the C/H ratio results. After 600°C all the aliphatic C-H were not observed in the IR spectra, suggesting a total loss of aliphatics. This was probably due to the fusion of the aromatic rings leading to a drastic loss of hydrogen observed from the C/H ratio.

3.4.4 Conclusions

The characterisation of the acidity of humic acids using IR techniques was not possible due to the interference caused by the functional groups of humic acids during the analysis. As a result no conclusions can be made regarding the type of acid sites as well as the acid strength using IR technique. However, the H^+ ions concentration determination used indicated an amount of these ions in humic acids comparable with those found in the zeolites used.

The influence of thermal treatment on the chemical structure of humic acids was demonstrated. It is concluded from the study that there was a change in the chemical structure that is associated with the loss of mass during thermal treatment of humic acids under N_2 atmosphere. There was a loss in functionality of the humic acids that accompanied the loss in mass with increase in temperature. The carboxylic acids were found to be easily affected by temperature, which gave rise to decarboxylation resulting in the loss of carboxylic acids.

Phenolic acid groups were found to be more stable against the increased temperatures. This was derived from the fact that the phenolic acid groups seemed to be lost at elevated temperatures of about 600°C. The loss of functionality was also confirmed with the results obtained from infrared spectra. It was also noted from the IR results that there seems to be a loss of aliphatic nature of the structure with the formation of a more aromatic structure, with increase in temperature. This was also confirmed by the associated increase in carbon/hydrogen ratio that was observed with the increased temperatures.

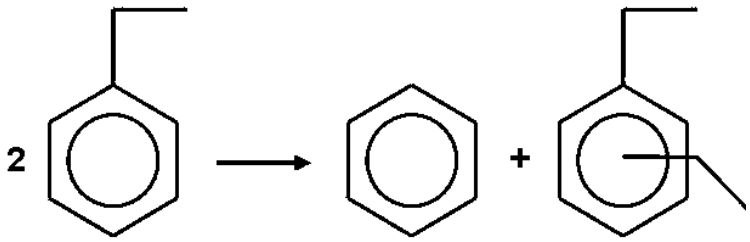
3.5 Test reaction: Ethylbenzene transformation over humic acids

3.5.1 Introduction

This section highlights the results obtained with test reaction on the transformation of ethylbenzene over humic acids as potential catalysts. The details of the experimental part are given in section 2.5.2.

3.5.2 Results and discussion

The attempted reaction was that of ethylbenzene disproportionation towards the formation of benzene and diethylbenzene, as shown in scheme 2.



Scheme 2: Ethyl benzene disproportionation.

With the reaction carried out at 180, 250 and 300°C no alkyl-transfer reaction products, i.e. benzene and diethylbenzene, were identified in the product streams. However there was a conversion of ethylbenzene towards the formation of other products such as styrene, 1-phenyl ethanol and 1-phenyl ethanone. The composition of the product stream is indicated in the table B1, B2 and B3.

The conversion of ethylbenzene (EB) was calculated using the equation:

$$\text{Ethylbenzene (EB) conversion\%} = [(EB_{(feed)} - EB_{(product)})/ EB_{(feed)}]$$

Samples were collected after every 30 minutes in order to monitor the catalysts activity with time on the stream. These reactions were carried out with the catalyst time in the

stream up to 3 hours. Each product sample was analysed using a GC-MS. Product molar compositions were calculated using the GC-MS results and these are indicated in table B1, B2 and B3. Conversions and product yields were calculated based on these results. The graph in Figure 3.20 depicts the behaviour of the conversion of ethylbenzene with time on stream at different temperatures.

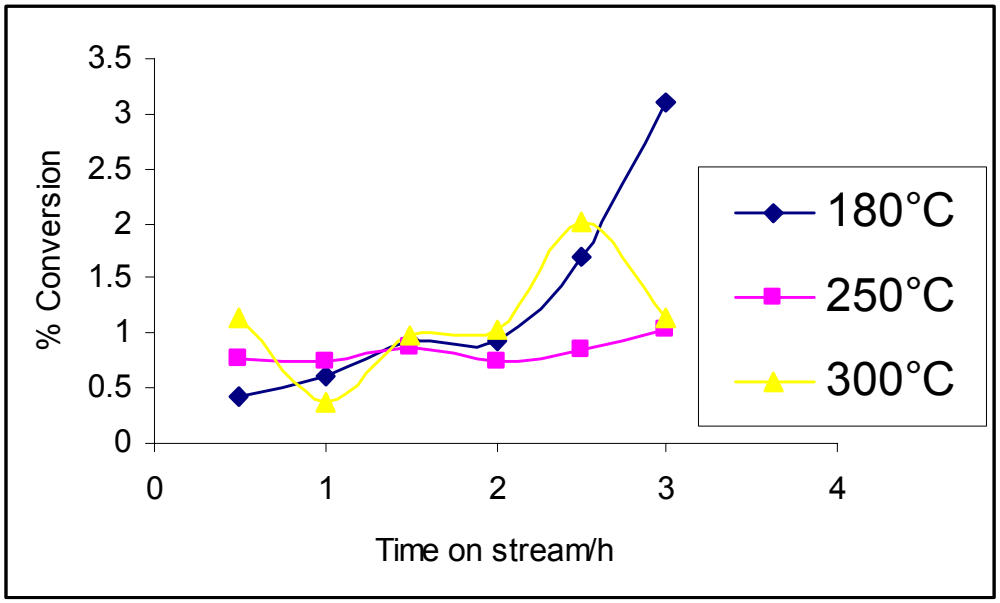


Fig 3.20: Ethylbenzene conversions at different temperatures

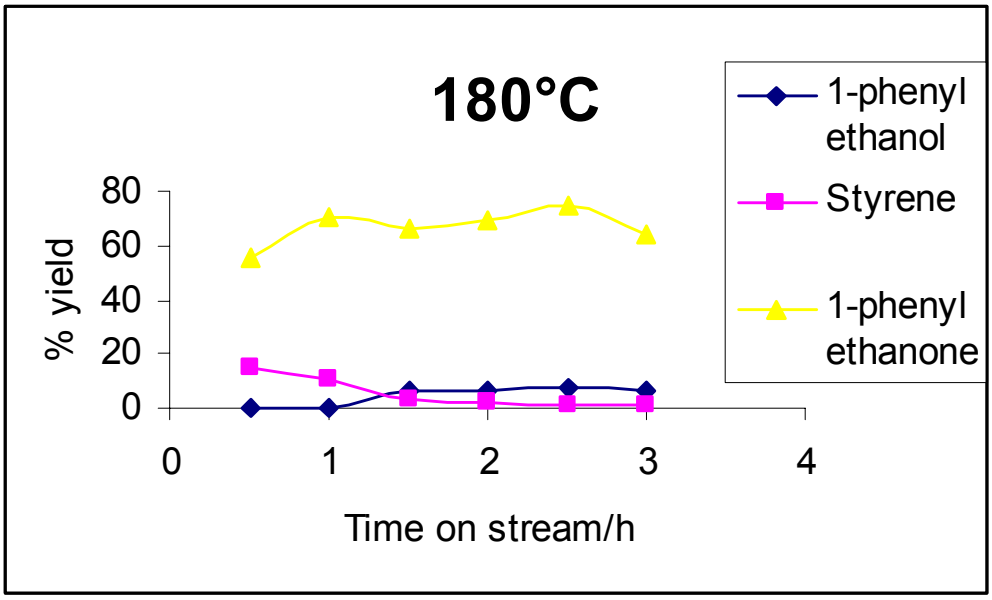
It is observed from this graph that very low conversions of ethylbenzene were achieved even at higher temperatures. This can be due to the weak acid site strength associated with the humic acids. In a study by de Vos et al. where disproportionation of ethylbenzene on LaNaY zeolites was carried out, conversions of around 5% were reported [27]. However, with the use of HY zeolites and mordenites higher conversions are achieved, with conversions as high as 50% reported [32].

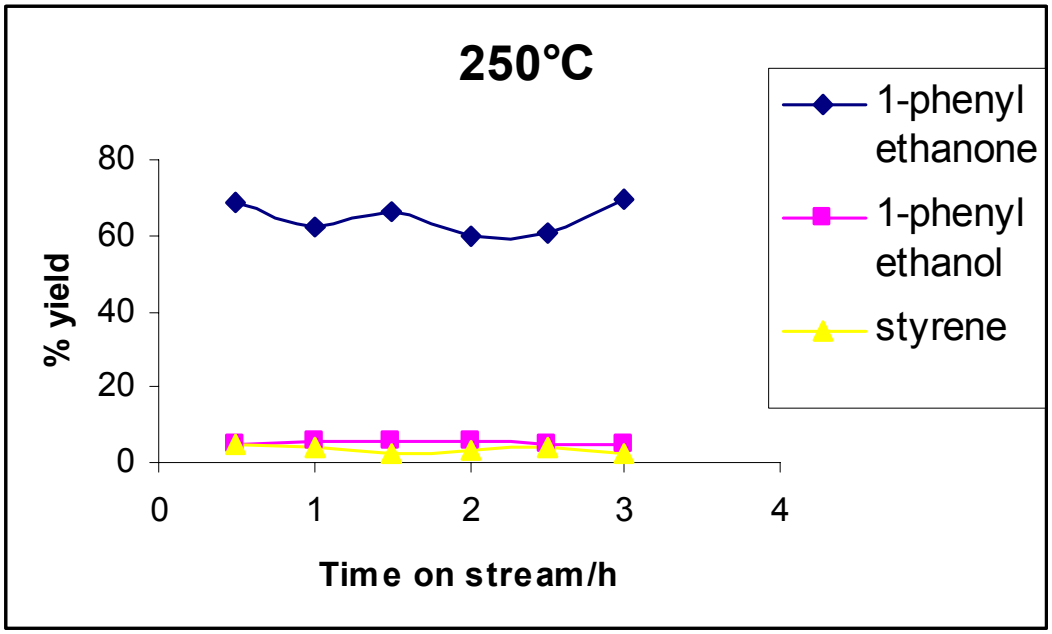
It was observed in the product stream that no benzene and diethylbenzene which are products of disproportionation were formed. However a slight increase in the amounts of 1-phenyl ethanol, 1-phenyl ethanone and styrene was observed. Of interest was the formation of styrene although in small amounts. The yields of these compounds were calculated with respect to the reacted ethylbenzene.

The equation used to calculate the yields is shown below:

$$\% \text{ yield} = [(\text{moles formed} \times \text{stoichiometric factor}) / EB_{(\text{reacted})}] \times 100$$

Figure 3.21 shows the yields of the products at different temperatures.





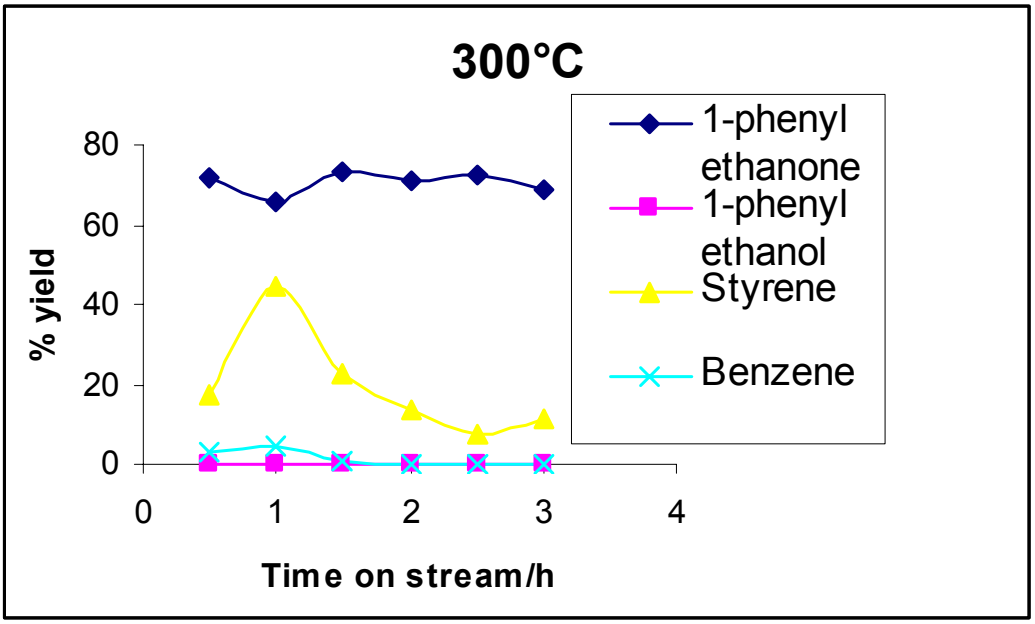
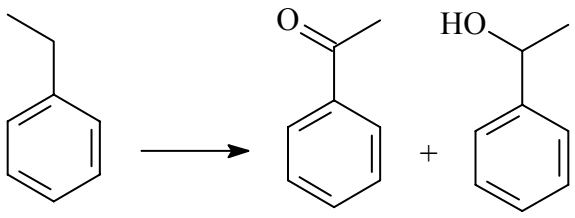


Fig 3.21: Yields of the products at different temperatures

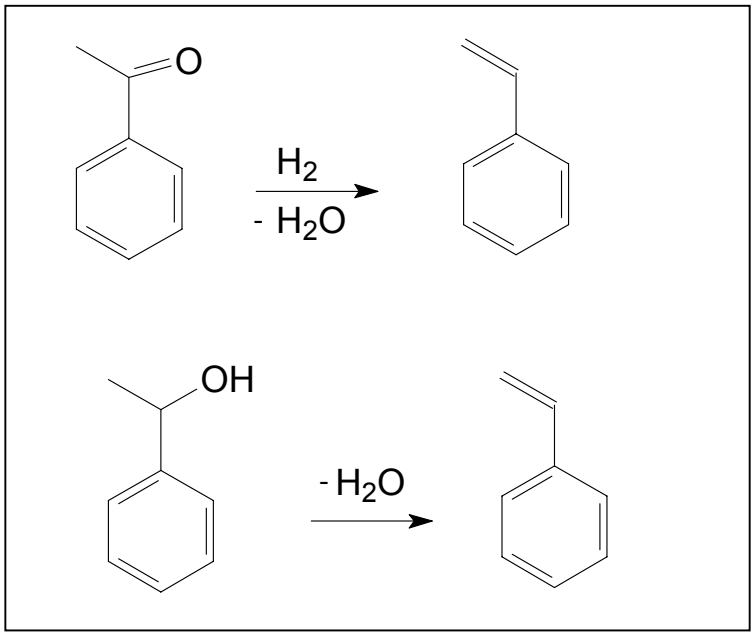
It is observed from the results that no disproportionation products were identified in the product streams for all the temperatures. However, small amounts of benzene were identified for the reactions at 300°C although this was observed in the first hour and a half, after which it disappeared and no diethylbenzene was observed. This suggested that the formation of benzene was due to ethylbenzene dealkylation rather than disproportionation.

It is interesting to see the formation of styrene in these reactions. It was noted that there was a high amount of styrene formed at 300°C after the first hour. This can be due to the oxidative dehydrogenation reactions of ethylbenzene induced by the catalyst. The ability of humic acids to catalyse these reactions was expected since they are catalysed by other carbon based catalysts such as activated carbons. Looking at the graph of the yield at 300°C, it can be deduced that styrene formed from 1-phenyl ethanone since the dip in the 1-phenyl ethanone plot was accompanied by a subsequent increase in the styrene yield. The conversion of ethylbenzene at the first hour was at the lowest for the 300°C results. This indicated that styrene was derived from the oxygenated molecules i.e. 1-phenyl ethanone and 1-phenyl ethanol. Also at 180°C there was a decrease in the styrene yield

which was accompanied by a subsequent increase in the yields of both 1-phenyl ethanol and 1-phenyl ethanone. This suggested that the conversion of ethylbenzene was towards the formation of 1-phenyl ethanol and 1-phenyl ethanone as shown in scheme 3, which are then converted through dehydrogenation to styrene (scheme 4).



Scheme 3: Formation of 1-phenyl ethanol and 1-phenyl ethanone from ethyl benzene.



Scheme 4: Stryrene formation from 1-phenyl ethanol and 1-phenyl ethanone

It is reported that for oxidative dehydrogenation to take place there must be an oxidizing agent. Oxygen and in some cases carbon dioxide was normally used [34,35,36]. In this case no oxygen or carbon dioxide was fed into the system, the oxidation agent could have been the carbon dioxide produced from the humic acids during the reaction. The

oxidation of the ethylbenzene leads to the formation of the oxygen bearing 1-phenyl ethanone and 1-phenyl ethanol as shown in scheme 4. These are further converted to styrene as shown in scheme 5.

3.5.3. Conclusions

The analysis of the products obtained indicated no formation of transalkylation products under the reaction conditions used. It can be deduced that no alkyl transfer reactions occurred on humic acids as catalysts but a conversion of the ethyl benzene towards the formation of other products was observed. The increased temperatures of the reaction did not have a great impact on ethylbenzene conversions for the reaction periods employed. The impact of temperature is rather observed with the product composition (selectivity) as observed by increased amount of styrene within the first hour and a half of the reaction carried out at 300°C. The formation of trace amounts of benzene at the first hour and a half at 300°C indicates the possibility of dealkylation taking place.

The formation of styrene in the product streams indicated the possibility of oxidative dehydrogenation of ethylbenzene to some extent. It can be concluded that, like other carbon materials such as activated carbon and coal, humic acids catalyst may be, to some extent, used for oxidative dehydrogenation.

Further work on the optimisation of the production of styrene from ethylbenzene using humic acids as catalysts can be of interest. It is well known that oxygenated aromatics in the impure feed are the cause of catalyst deactivation for zeolites. It will be interesting to carry out an investigation on the deactivation of humic acids, by allowing longer reaction times and also by comparing with purified feed. This will help in establishing the catalyst lifetime of humic acids as well as factors that lead to catalyst deactivation.

CHAPTER 4: CONCLUSIONS AND RECOMMENDATIONS OF THE STUDY

The study undertaken was aimed at the optimisation of humic acids production as well as the evaluation of these as potential acid catalysts for transalkylation. Air oxidation was used for the selection of a coal type, where it was illustrated that coal with high vitrinite content showed good reactivity and are favoured for the production of humic acids through oxidation. However the yields of the products were too low to continue with the method, hence slurry phase oxidation was used to optimise the oxidation. Slurry phase oxidation showed a much improved oxidation with increase in the extent of oxidation and oxidation products observed. The highest oxidation using slurry phase oxidation method was obtained at the temperature of 180°C and a pressure of 40 bar. There was also the highest yield of humic acids obtained at these conditions.

Acidity characterisation on humic acids using IR techniques was found to be difficult due to the interference with the analysis of the functional groups in humic acids but zeolites were analysed successfully. The use of methods other than IR techniques for analysis of the acidity of humic acids is recommended. Analysis of the concentration of H^+ ions showed that humic acids have comparable amounts of H^+ ions to those of zeolites; but the difference in strengths and characteristics of acid sites was not quantified.

Thermal analysis on humic acids indicated that humic acids were stable up 300°C and above this temperature a loss of mass is experienced. Carboxylic acids were removable at low temperatures just above 300°C, but phenolic acid groups were stable up to 600°C.

Test reactions of ethylbenzene disproportionation over humic acids indicated their inability to induce transalkylation reactions, with the oxidative dehydrogenation of ethylbenzene being the reaction that was likely to be taking place. Dealkylation of ethylbenzene was observed for the reactions carried out at 300°C for an hour and a half. Further work on the optimisation of the production of styrene from ethylbenzene using humic acids as catalysts can be of interest. It is well known that oxygenated aromatics in

the impure feed are the cause of catalyst deactivation for zeolites. Thus, it will be interesting to carry out an investigation on the deactivation of humic acids, by allowing longer reaction times and also by using purified feed. This will help in establishing the catalyst lifetime of humic acids as well as factors that leads to catalyst deactivation, and using pure feed may confirm the oxidative dehydrogenation observed.

APPENDICES

Appendix A.

Table A1: Yields of the extracted humic acids

Coal	Reaction Time/h	Reaction Temperature/°C	mass of HA extracted	% H.A (w.r.t oxidised coal)
Waterberg	3.25	150	0.19	1.9
Waterberg	19	150	0.31	3.1
Waterberg	43	150	0.37	3.7
Waterberg	139	150	0.37	3.7
Waterberg	235	150	0.41	4.1
Waterberg	379	150	0.65	6.5
Twistdraai	379	150	0.59	5.9
Syferfontein	379	150	0.27	2.7

Table A2: Results of the slurry phase oxidation.

Oxidation temperature/°C	unoxidized	120	140	160	180	200
Oxidized coal						
mass (g)	420	386	393	394	388	380
% moisture	9.08	1.74	2.17	2.16	0.87	1.31
%ash	4.16	9.85	10.57	10.47	10.31	11.2
%C	70.91	68.04	69.4	64.71	57.37	56.56
%O	8.77	13.95	11.04	16.19	19.01	21.61
Fulvic acids						
mass(g)	0	0	2.011	2.11	2.78	3
mass%	0	0	0.48	0.50	0.66	0.71
%C	0	0	0.44	6.03	10.83	11.2
%C(CO2 + CO)	0	2.87	1.07	0.17	2.71	3.15
humic acids						
mass(g)	0	0.28	0.34	0.2	6.13	4.16
mass%	0	2.8	3.4	2	61.36	41.6

Table A3: Functional groups determination for slurry phase oxidation

Oxidation temperature/°C	unoxidized	120	140	160	180	200
Total acids						
mass(g)	1.01	1	1.02	0.99	1.02	1
Vs(ml)	13	11.59	10.58	7.58	3.38	3.25
Vb(ml)	14.07	14.07	14.07	14.07	14.07	14.07
Total acids(meq/g of C)	**0.76**	**1.66**	**2.36**	**4.2**	**6.13**	**6.12**
Carboxylic acids						
mass(g)	0.35	0.3	0.311	0.301	0.3	0.35
Vs(ml)	2	2.45	3.25	14.12	16	29.55
Vb(ml)	0.85	0.85	0.85	0.85	0.85	0.85
Carboxylic acids(meq/g of C)	**0.05**	**0.07**	**0.1**	**0.55**	**0.58**	**0.93**
Phenolic acids(meq/gC)	**0.71**	**1.59**	**2.26**	**3.65**	**5.55**	**5.19**
phenolic/carboxylic	**14.20**	**22.71**	**22.60**	**6.64**	**9.57**	**5.58**

Table A4: Integral results of Lewis and Brønsted acid sites

Sample	Brønsted /mg	Lewis /mg	B/L ratio
H-Mordenite	0.22	0.02	11
H-Y Zeolite	0.52	0.44	1.18

Appendix B

Table B1: Reaction at 180°C

Reaction time /h / Composition/ mol%	Fresh/00	0.5	1	1.5	2	2.5	3
Ethylbenzene	**91.57**	**91.19**	**91.02**	**90.73**	**90.73**	**90.03**	**88.70**
1-phenyl ethanol	**0.16**	**0.13**	**0.16**	**0.21**	**0.22**	**0.28**	**0.34**
1-phenyl ethanone	**2.14**	**2.37**	**2.54**	**2.71**	**2.73**	**3.30**	**3.94**
Styrene	**0.00**	**0.06**	**0.06**	**0.03**	**0.02**	**0.01**	**0.02**
Benzene	**0.00**	**0.00**	**0.00**	**0.00**	**0.00**	**0.00**	**0.00**
Others	**6.13**	**6.25**	**6.22**	**6.23**	**6.30**	**6.36**	**7**

Table B2: Reaction at 250°C

Reaction time /h / Composition/ mol%	Fresh/00	0.5	1	1.5	2	2.5	3
Ethylbenzene	**91.57**	**90.86**	**90.89**	**90.77**	**90.88**	**90.81**	**90.63**
1-phenyl ethanol	**0.16**	**0.2**	**0.2**	**0.21**	**0.2**	**0.2**	**0.21**
1-phenyl ethanone	**2.14**	**2.64**	**2.57**	**2.68**	**2.56**	**2.61**	**2.81**
Styrene	**0.00**	**0.04**	**0.03**	**0.02**	**0.02**	**0.03**	**0.03**
Benzene	**0.00**	**0.00**	**0.00**	**0.00**	**0.00**	**0.00**	**0.00**
Others	**6.13**	**6.26**	**6.31**	**6.32**	**6.34**	**6.35**	**6.32**

Table B3: Reaction at 300°C

Reaction time /h / Composition/ mol%	Fresh/00	0.5	1	1.5	2	2.5	3
Ethylbenzene	**91.57**	**90.54**	**91.24**	**90.66**	**90.62**	**89.72**	**90.28**
1-phenyl ethanol	**0.16**	**0.03**	**0.02**	**0.01**	**0.07**	**0.07**	**0.08**
1-phenyl ethanone	**2.14**	**2.89**	**2.37**	**2.81**	**2.83**	**3.5**	**3.04**
Styrene	**0.00**	**0.18**	**0.15**	**0.2**	**0.13**	**0.15**	**0.15**
Benzene	**0.00**	**0.03**	**0.01**	**0.01**	**0.00**	**0.00**	**0.00**
Others	**6.13**	**6.33**	**6.21**	**6.31**	**6.35**	**6.56**	**6.45**

APPENDIX C

Determination of the amount of H+ ions per gram of a dry resin

Weigh out accurately a four to six gram sample of the conditioned resin. Transfer the sample to a short stemmed 600ml funnel containing a filter paper of medium porosity. (At the same time, weigh out a second sample of conditioned resin for solids determination. The solids determination is performed by weighing the sample, then drying it in an oven at 105 to 115°C overnight and determining the dry weight of the resin). Allow about one-half litre of deionised water to pass through the sample slowly and then allow the resin to drain. Support the funnel in a one litre volumetric flask and above this suspend a separator funnel containing four percent neutral sodium sulphate solution. This solution is allowed to percolate through the resin sample over a period of one hour to fill the separatory funnel to exactly one litre. During the passage of the sodium sulphate solution, it is important that the solution level be kept slightly above the

top level of the resin. Aliquots of 100 ml are taken from this effluent solution for titration with standard 0.1 N potassium hydroxide, using phenol-phthalein as the indicator. Results are calculated as mill equivalents per gram dry resin as follows:

Capacity Calculation

$$\frac{V\,(KOH) \times N\,(KOH)}{\text{Sample weight} \times \frac{\text{percent solids}}{100}} = \frac{\text{meq. of } H^{+} \text{ ions}}{\text{gram of dry resin}}$$

Solids calculation

$$\frac{\text{Weight of dry resin} \times 100}{\text{Weight of conditioned resin}} = \text{percentage solids}$$

If the resin sample used in the capacity determination is thoroughly dried, it should be hydrated in deionised water for approximately 30 minutes before passage of the sodium sulphate solution through it. The percent solids factor in the capacity equation given will be unity for a dry resin.

REFERENCES

1. S.M. Al-Zahran, M.C. Al-Kinary, K.I Al-Humanaizi and S.H. Al-Khowaiter, *Chemical Engineering and Processing*, 41, **2002**, 321-327
2 X. Rozanska, X. Saintigny, R.A. van Santen and F. Hutscchka, *Journal of Catalysis*, 202, **2001**, 141-155.
3 L. Forni, G. Cremona, F. Missineo, G. Bellusi, C. Perego and G. Pazzuconi, *Applied Catalysis A: General*, 121 issue 2, **1995**, 261-272.
4 Guisnet M. R., *Acc. Chem. Res*., Vol. 23, No. 11, **1990**, 392-398
5 Molecular structure of humic acids, Stevenson F. J., **1982**, www. richeart.net/molecular_structure_of_humic_acids.htm
6 Erth G., Knozinger H., Weitkamp J., *Handbook of Heterogeneous Catalysis*, Vol. 3, Weinheim: VCH, **1997**, 1123-1137
7 S.L. Meisel, J.P. McCollough, C.H. Lechthaler, *CHEM-TECH*, **1976**, 6, 86.
8 Breck, D. W., *Zeolite Molecular Sieves*, *Kriger*: Malabar F. L., **1984**; Barrer R. M., *Zeolites and Clay Minerals as Sorbents and Molecular Sieves*; Academic Press: New York, **1978**.
9 van Krevelen D.W., *Coal Science and Technology*, 3, **1981**, 219-237
10 Lawson G.J., Stewart D., *Humic Substances II, Coal Humic acids*, John Wiley & Sons, Ch 23, **1989**, 641- 677.
11 Stevenson F.J., *Humus Chemistry: Genesis, Composition, Reactions*, 2, John Wiley & Sons Inc. **1994**, 188- 211.
12 Louwenhaupt D.E., Gray R.J., *International Journal of Coal Geology*, 1, **1980**, 63-73.
13 Dekker J., Cronje I. J.,Louwrens H.B., Swart H., Non-catalytic oxidation of water slurried coal with oxygen: A promising new route to oxihumic and oxifluvic acids*, In proceedings of the Seventh Annual International Coal Conference,* University of Pittsburg, Pittsburg, PA, **1990**, 703-708.
14 Rousa R., Girardi E., Calemma V., *Humic acids from coal. Production, characterization, and utilization*. Elsevier Science **1994**, 1225-1244.

15 Friedman, L.D., and Kinney, C.R.. *Humic acids from coal. Controlled air oxidation of coal and carbons at 150°C to 400°C.* Ind. Eng. Chem., 42, **1950,**2525-2529

16 England T., Hand P.E., Michael D. C., Falcon L.M., Yell A.D., *Coal Preparation in South Africa*, 4th edit., South African Coal Processing Society, **2002**, 1-13

17 Ashmin K.B., Debapriya C., Samar S. C., *Chemical changes accompanying oxygenation of coal by air and deoxygenation of oxidized coal by thermal treatement,* **1988**, 1129-1133

18 Monika Kurková, Zdenek Klika, Christiana Kliková and Josef Havel, *Chemosphere,* Volume 54, Issue 8, February **2004**, Pages 1237-1245

19 Itay M., Hill C.R., Glasser D., *A study of the low temperature Oxidation of coal*, Fuel Processing and Technology, 21, **1989**, 81-97

20 Louwrens B. H., *Optimalisering van die oksidatiewe omsetting van steenkool*, **1989**, BSc Honours thesis, University of Potchefstroom

21 Schnitzer M., Khan S.U (Eds)., *Humic Substances in the Environment,* Marcel Dekker*,* **1972**, 203- 251

22 Louwrens B. H.*, 'n ondersoek na die prosesmeganisme en lewengvastbaarheid van die natfase steenkooloksidasieroete*, **1992**, MSc (Chem), thesis, University of Potchefstroom

23 Dekker J., Cronje I. J.,Louwrens H.B., Swart H., *Non-catalytic oxidation of water slurried coal with oxygen: A promising new route to oxihumic and oxifluvic acids. In proceedings of the Seventh Annual International Coal Conference,* University of Pittsburg, Pittsburg, PA **1990**, 703-708

24 Bergh J. J., Cronje I. J., Dekker J., Dekker T.G., Gerritsma M., Mienie L.J., *Fuel*, 76, No. 2, **1997**, 149-154

25 Lawson G.J., Stewart D., *Humic Substances II, Coal Humic acids*, Ch 23, John Wiley & Sons **1989**, 641-677

26 Tiako Ngandjui L.M.T., Louhibi D., Thyrion F.C., *Chemical Engineering and Processing* 36, **1997**, 133-141

27 Standard Reaction for Acidity Characterization Ethylbenzene Disproportionation, *July 31, 2002* http://www.iza-catalysis.org/EB_Disprop.html

28 Mavrodinova V., Popova M., Pal Borbely G., Mihalyi R.M., Minchev Ch., *Applied Catalysis A: General* 248 **2003**, 181-196

29 Moreau F., Gnep N. S., Lacombe S., Merlen E. and Guisnet M., *Applied Catalysis A: General, Volume 230, Issues 1-2, 30 April **2002**, Pages 253-262*

30 Moreau F., Bernard S., Gnep N. S., Lacombe S., Merlen E. and Guisnet M., *Journal of Catalysis, Volume 202, Issue 2,10 September**2001**,Pages402-412*

31 Rousa R., Girardi E., Calemma V., *Humic acids from coal. Production, characterization, and utilization*. Elsevier Science, **1994**, 1225-1244

32 Karge, H.G.; Ladebeck, J.; Sarback, Z.; and Hatada, K.; Conversion of alkyl benzenes over zeolites catalysts. I. Dealkylation and disproportionation of alkylbenzene over mordenites, *Zeolites*, 2, **1982**,94

33 Karge, H.G.; Hatada, K.; Zheng, Y.; and Fiedorow, R., Conversion of alkyl benzenes over zeolites catalysts. II Disproportionation of diethylbenzene over Faujasite-type zeolites, *Zeolites*, 3, **1983**,13

34 Dziembaj R.; Kustrowski P.; Chmielarz L.; App. Cat. A: General 255 (2003) 35-43.

35 Fiedorow R.; Fra□ski R.; Krawczyk A.; and Beszterda S.; *Journal of Physics and Chemistry of Solids*, 65, Issues 2-3 , **2004**, 627-632.

36 Sakurai Y.; Suzaki T.; Ikenaga N.; and Suzukin T, *Applied Catalysis A: General* 192, Issue 2 , **2000**, 281-288

37 Dziewi~cki Z.; Jagie□o M.; and Makowski A.; *Reactive and Functional Polymers* 33, Issues 2-3 , **1997**,185-191.

38 Grunewald G. C.; and Drago R. S. *Journal of Molecular Catalysis* 58, Issue 2 , **1990**, 227-233.

39 Maldonaldo-Hodar, F.J.; Madeira, L.M.; Portela, M.F.; *App. Cat. A, Genaral*, 178, **1998**, 46-60.

40 Perreira, M.F.R.; Orfao, J. J. M.; Figueiredo, J.L.; *App. Cat. A: General* 184, **1999,** 153-160.

41 Perreira, M.F.R.; Orfao, J. J. M.; Figueiredo, J.L.; *App. Cat. A: General* 218, **2001,** 307-318.

42 Perreira, M.F.R.; Orfao, J. J. M.; Figueiredo, J.L.; *Colloids and Surfaces A: Physicochem. Eng. Aspect*s. In press Corrected proof, available online (**2004**).

43 Lu X.Q., Vassallo A.M., Johnson W.D., *Journal of Analytical and Applied Pyrolysis*, 43 **1997**, 103-114

44 Mangrich A.S., Lobo M.A., Tanck C.B., Wypych F., Toledo E.B.S., Guimaraes E., *J. Braz. Chem. Soc*. Vol. 11 n.2, April **2000**

45 Arenillas A., Rubiera F., Pis J.J., *Journal of Analytical and Applied Pyrolysis*, 50, **1999**, 31-46

46 Khabtou S., Chevreau T., Lavalley J. C., *Microporoous Materials*, 3, **1994**, 133-148